




Entropy Stable and Well-Balanced Discontinuous Galerkin Methods for the Nonlinear Shallow Water Equations

Xiao Wen¹ · Wai Sun Don² · Zhen Gao² · Yulong Xing³ 

Received: 31 December 2019 / Revised: 24 April 2020 / Accepted: 1 June 2020
© Springer Science+Business Media, LLC, part of Springer Nature 2020

Abstract

The nonlinear shallow water equations (SWEs) are widely used to model the unsteady water flows in rivers and coastal areas, with extensive applications in ocean and hydraulic engineering. In this work, we propose entropy stable, well-balanced and positivity-preserving discontinuous Galerkin (DG) methods, under arbitrary choices of quadrature rules, for the SWEs with a non-flat bottom topography. In Chan (J Comput Phys 362:346–374, 2018), a SBP-like differentiation operator was introduced to construct the discretely entropy conservative DG methods. We extend this idea to the SWEs and establish an entropy stable scheme by adding additional dissipative terms. Careful approximation of the source term is included to ensure the well-balanced property of the resulting method. A simple positivity-preserving limiter, compatible with the entropy stable property, is included to guarantee the non-negative water heights during the computation. One- and two-dimensional numerical experiments are presented to demonstrate the performance of the proposed methods.

Keywords Discontinuous Galerkin methods · Shallow water equations · Entropy stable · Entropy conservative · Well-balanced property · Positivity-preserving limiter

1 Introduction

The nonlinear shallow water system is a mathematical model for the fluid movement in various shallow water environments, where the water depth is much smaller than the charac-

✉ Yulong Xing
xing.205@osu.edu

Xiao Wen
xiaowen_ouc@163.com

Wai Sun Don
donwaisun@outlook.com

Zhen Gao
zhengao@ouc.edu.cn

¹ College of Oceanic and Atmospheric Sciences, Ocean University of China, Qingdao, China

² School of Mathematical Sciences, Ocean University of China, Qingdao, China

³ Department of Mathematics, Ohio State University, Columbus, OH 43210, USA

teristic wave length. It has been widely used in the earth's atmosphere, ocean, environment, water engineering and the development and utilization of clean energy, such as tsunami and storm surge prediction, sediment and pollutant transfer, tidal energy capture in estuaries and offshore waters. In two-dimensional setting, the shallow water equations (SWEs) include the governing equations of the water height h and the momentums, taking the form of

$$\begin{cases} h_t + (hu)_x + (hv)_y = 0, \\ (hu)_t + \left(hu^2 + \frac{1}{2}gh^2\right)_x + (huv)_y = -ghb_x, \\ (hv)_t + (huv)_x + \left(hv^2 + \frac{1}{2}gh^2\right)_y = -ghb_y, \end{cases} \quad (1.1)$$

where $(u, v)^T$ is the velocity vector, $b(x, y)$ represents the bottom topography and g is the gravitational constant.

All types of numerical methods, including finite volume, finite difference, and finite element methods have been presented for the SWEs. In this paper, we will confine our attention in the high order finite element discontinuous Galerkin (DG) methods. The DG methods belong to a class of finite element methods, which use discontinuous piecewise polynomial space as the solution and test function spaces (see [13] for a historic review). The DG methods hold several advantages, including the high order accuracy, local conservativity, flexibility for hp -adaptivity, easy handling of complicated geometries, and highly efficient parallel implementations. It has been used extensively in solving the SWEs [16,17,23,31] since the early 2000's.

SWEs with a non-flat bottom topography belong to the family of hyperbolic balance laws. This type of models admit steady state solutions, in which the flux gradients are exactly balanced by the source term. To capture these steady state solutions or the small perturbations of them, traditional numerical schemes cannot exactly balance the flux gradients and the source term in the discrete level, and may introduce spurious oscillations. Well-balanced methods [4] are designed to preserve exactly these steady state solutions up to machine error with relatively coarse meshes. For the SWEs, the still-water steady state solution taking the form of

$$u = v = 0, \quad \text{and} \quad h + b = \text{const}, \quad (1.2)$$

is often considered in the applications. Many well-balanced methods [2,4,19,28,29,38,39,41] have been studied, and we refer to the survey paper [45] for a complete list of existing literatures on this topic. On the other hand, the dry areas might appear in the natural environments such as the dam-breaking problem over a dry land. Special attention needs to be paid near the wetting and drying front, as the non-physical negative water height may be generated numerically in the simulations when using high order schemes. This may cause problems in calculating the eigenvalues and renders the system neither hyperbolic nor well posed. Many positivity-preserving schemes [3,6,7,20] were designed to preserve the positivity of the water height. A few existing numerical methods [1,18,27,35,43,44] are able to maintain both well-balanced and positivity-preserving properties at the same time.

For the hyperbolic balance laws including the SWEs, discontinuous solutions may appear in finite time even with smooth initial conditions, which leads to the definition of weak solutions. However these weak solutions could be non-unique. In order to find the unique, physically relevant entropy solution from all the weak solutions, the second law of thermodynamics is imposed as the admissibility criterion, which can be interpreted as entropy conditions in the form of entropy functions. Entropy stable methods refer to numerical meth-

ods which can satisfy entropy inequalities in the discrete level. There have been tremendous works on designing entropy stable methods for the system of hyperbolic conservation laws, and we refer to a comprehensive survey [34] by Tadmor on this topic. The classic DG method is known to satisfy a discrete entropy inequality, for the square entropy only and when the conservation laws is scalar or symmetric system [25]. Recently, there have been many works [8,9,11,22,37] on designing high order entropy stable DG methods. Most of these methods are based on the recast of the DG methods in the nodal formulation [24,26]. One difficulty in proving these entropy inequalities is that the integration by parts (IBP) property may not hold any more, when the quadrature rules are used to approximate the integrals in the implementation. It was shown in [21] that, with the choice of Gauss–Lobatto quadrature points, the corresponding discrete derivative operators satisfy the summation-by-parts (SBP) property, an analogue of the IBP property. High order entropy stable and well-balanced nodal DG methods are then designed for the SWEs in [22] based on a split formulation of the model, which deals with the loss of chain rule in the discretization. The extension to two-dimensional SWEs on unstructured curvilinear meshes is investigated in [37], and this method has been combined with a positivity-preserving limiter and implemented on GPUs in [36]. In [11], a unified framework of entropy stable high order nodal DG schemes has been constructed. They demonstrated that, by introducing a special quadrature rule, the formulation of SBP operators can be deduced even on the triangular meshes, which leads to an easy extension of entropy stable nodal DG methods to unstructured triangular meshes. More recently, a generalization of discretely entropy conservative methods was extended from diagonal-norm SBP DG methods to a more general class of high order DG methods under arbitrary choices of volume and surface quadrature rules in [9]. The differences between the sensitivity of methods based on Gauss–Lobatto quadrature and methods based on Gauss quadrature rules have also been studied. We refer to [12] for a recent review paper on discussion of these entropy stable DG methods and more references in this area.

In this paper, we propose entropy stable, well-balanced and positivity-preserving DG methods on Gauss quadrature rules for the SWEs with a non-flat bottom topography, by extending the entropy conservative and entropy stable schemes presented in [9]. The main contribution of this work is to demonstrate that the proposed entropy stable methods, coupled with suitable source term approximation, satisfy both well-balanced and positivity-preserving properties when the non-flat bottom topography is considered in the model. The entropy stable scheme are constructed by adding additional dissipative terms to the entropy conservative scheme. We provide a complete proof to show that the entropy inequality (now with the bottom topography term) can be preserved in the discrete level, following that in [9]. The local conservation property of the proposed DG methods has also been proven. To achieve well-balanced property, we propose to use the same derivative operator to discretize the source term, and demonstrate that the approximation of the flux gradient and the source term exactly balance each other in the discrete level. To ensure the positivity-preserving property, we first demonstrate that the positive cell average of water height is maintained under a suitable CFL condition, and then incorporate the positivity-preserving limiter proposed in [43] for the SWEs to ensure that the solution is positive everywhere in the domain. In addition, it is shown that the positivity-preserving limiter itself does not increase entropy and is compatible with entropy stable methods. Similar results on the positivity-preserving limiter have also been studied in [30,36] for their entropy stable methods. One-dimensional SWEs is considered first to present the proposed entropy stable, well-balanced and positivity-preserving methods, and their extension to two-dimensional problem on rectangular meshes is also provided. High order entropy stable, well-balanced and positivity-preserving nodal DG methods were also presented in [36,37] for the SWEs. Compared with these works, the proposed method is based

on the modal formulations and allows arbitrary choices of volume and surface quadrature rules, with the possibility of attaining better accuracy with smaller degrees of freedom. Also, different dissipation terms were introduced to derive entropy stable methods. Although derived from different motivation, the well-balanced technique presented here also involves the approximation of the source term in both volume integral and interface terms. To achieve the positivity-preserving property, all of these works extend the same positivity-preserving limiter proposed in [43] for the SWEs. Only the rectangular meshes in two-dimensional setting are considered in this paper as a first step to illustrate the idea, and our future work involves the extension of these methods to curvilinear grids and triangular grids.

The paper is organized as follows. In Sect. 2, a brief review of the entropy conservative and discretely entropy conservative schemes is provided. Section 3 starts with the construction of entropy conservative methods for the one-dimensional SWEs with a non-flat bottom. Entropy stable, well-balanced, and positivity-preserving properties will be demonstrated. Section 4 presents the entropy stable DG scheme for the two-dimensional SWEs. We note that, for simplicity and clarity of presentation, all the proofs are only provided in one dimension, but the extension to two-dimensional problems on rectangular meshes is straightforward. In Sect. 5, some classical one-dimensional and two-dimensional numerical examples are presented to validate the proposed DG methods. Conclusions are given in Sect. 6.

2 On Discretely Entropy Conservation DG Methods

In this section, we first review the basic theory of the entropy conservation for hyperbolic conservation laws, and then discuss the entropy conservative DG schemes studied in [9,10].

2.1 Entropy Solutions of Hyperbolic PDEs

We consider the system of nonlinear conservation laws in one dimension with n variables

$$\frac{\partial \mathbf{Q}}{\partial t} + \frac{\partial \mathbf{f}(\mathbf{Q})}{\partial x} = 0, \quad (2.1)$$

where $\mathbf{Q} = (Q_1, Q_2, \dots, Q_n)^T$ is the unknown vector function and $\mathbf{f}(\mathbf{Q})$ is the flux function. The Jacobian matrix is defined as

$$\left(\mathbf{A}(\mathbf{Q}) \right)_{ij} = \frac{\partial f_i(\mathbf{Q})}{\partial Q_j}. \quad (2.2)$$

A convex function $U(\mathbf{Q})$ is said to be an entropy function for (2.1) if there exists the function $F(\mathbf{Q})$, called entropy fluxes, such that the following integrability condition holds

$$U'(\mathbf{Q}) \frac{\partial \mathbf{f}}{\partial \mathbf{Q}} = \frac{\partial F(\mathbf{Q})}{\partial \mathbf{Q}}, \quad (2.3)$$

where $U'(\mathbf{Q})$ means the derivative of $U(\mathbf{Q})$ with respect to \mathbf{Q} . We denote the entropy variables by $\mathbf{e} = U'(\mathbf{Q})$, and the entropy potential function ψ by

$$\psi(\mathbf{e}) = \mathbf{e}^T \mathbf{f}(\mathbf{Q}(\mathbf{e})) - F(\mathbf{Q}(\mathbf{e})), \quad (2.4)$$

which satisfies

$$\psi'(\mathbf{e}) = \mathbf{f}(\mathbf{Q}(\mathbf{e})).$$

In the smooth regions, we can multiply (2.1) on the left by $\mathbf{e}^T = U'(\mathbf{Q})^T$, and obtain the conservation of entropy

$$\frac{\partial U(\mathbf{Q})}{\partial t} + \frac{\partial F(\mathbf{Q})}{\partial x} = 0, \tag{2.5}$$

following the definition of the entropy flux. When the solution contains discontinuity, we require the entropy to dissipate, which leads to the following definition.

Definition 1 A weak solution \mathbf{Q} of (2.1) is called an entropy solution, if for all entropy functions U ,

$$\frac{\partial U(\mathbf{Q})}{\partial t} + \frac{\partial F(\mathbf{Q})}{\partial x} \leq 0, \tag{2.6}$$

holds in the sense of distribution.

Entropy stable method refers to numerical method which can satisfy the integral version of the entropy inequality (2.6) in the discrete level.

2.2 Notations

We start by introducing some necessary notations. Let's decompose the domain Ω into non-overlapping elements Ω^k of size h_k . We denote the maximal mesh size as $h = \max_{1 \leq j \leq K} h_j$. The piecewise polynomial space V_h is defined as

$$V_h = \left\{ v : v|_{\Omega^k} \in P^N(\Omega^k), \text{ in each element } \Omega^k \right\}, \tag{2.7}$$

where $P^N(\Omega^k)$ denotes the space of polynomials of degree N on the cell Ω^k .

The L^2 norm and inner products over the element Ω^k and the surface of the element $\partial\Omega^k$ are defined as

$$(Q, W)_{\Omega^k} = \int_{\Omega^k} Q(s)W(s)ds, \quad \|Q\|_{\Omega^k}^2 = (Q, Q)_{\Omega^k}, \quad \langle Q, W \rangle_{\partial\Omega^k} = \int_{\partial\Omega^k} Q(s)W(s)ds.$$

We also define the local L^2 projection operator $\mathbb{P}: L^2(\Omega^k) \rightarrow P^N(\Omega^k)$ such that

$$(\mathbb{P}Q, W)_{\Omega^k} = (Q, W)_{\Omega^k}, \quad \forall W \in P^N(\Omega^k).$$

The projection error operator \mathcal{E} of the variable Q is defined as

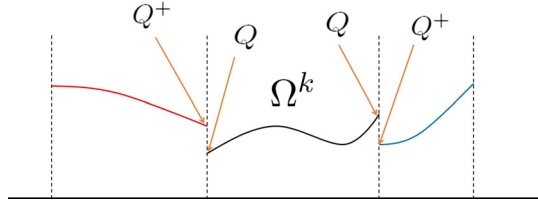
$$\mathcal{E}(Q) = Q - \mathbb{P}Q.$$

Since the approximation solution is allowed to be discontinuous at the cell interface, we denote $Q^+(x_{k+1/2})$ as the values of Q at $x_{k+1/2}$ evaluated on the neighboring elements, see Fig. 1 for the illustration. At the domain boundary, we have $Q^+(x_{k+1/2}) = Q(x_{k+1/2})$. We denote $[[Q]]_{k+1/2} = Q^+(x_{k+1/2}) - Q(x_{k+1/2})$ and $\{Q\}_{k+1/2} = (Q^+(x_{k+1/2}) + Q(x_{k+1/2}))/2$ as the jump and the average of Q at the cell interface $x_{k+1/2}$. n_x denotes the x -component of the outward normal vector.

2.3 Entropy Conservative DG Methods

In this subsection, the summary of the entropy conservation DG methods in [10, Sects. 3, 4] will be provided, and we refer to [10, Sects. 3, 4] for the details.

Fig. 1 The definition of Q^+ on the cell interfaces



The entropy conservative and entropy stable fluxes proposed by Tadmor [32,33] are defined as follows:

Definition 2 Let $\mathbf{f}_S(\mathbf{Q}_l, \mathbf{Q}_r)$ be a consistent and symmetric numerical flux. It is entropy conservative if

$$(\mathbf{e}_l - \mathbf{e}_r)^T \mathbf{f}_S(\mathbf{Q}_l, \mathbf{Q}_r) = \psi_l - \psi_r, \tag{2.8}$$

holds for the entropy variables $\mathbf{e}_j = \mathbf{e}(\mathbf{Q}_j)$ and the scalar entropy potential $\psi_j = \psi(\mathbf{e}(\mathbf{Q}_j))$, $j = r, l$. Similarly, the numerical flux $\mathbf{f}_S(\mathbf{Q}_l, \mathbf{Q}_r)$ is entropy stable if $(\mathbf{e}_l - \mathbf{e}_r)^T \mathbf{f}_S(\mathbf{Q}_l, \mathbf{Q}_r) \leq \psi_l - \psi_r$.

The following discrete numerical derivative operator is introduced in [10], which is one of the key components in designing entropy conservative methods.

Definition 3 Let $W(x)$ be a bounded function on each element Ω^k . Define $D_h^x : H^1(\Omega_h) \rightarrow V_h$ as the operator which satisfies

$$\begin{aligned} & (D_h^x Q, W\omega)_\Omega \\ &= \sum_k \left[\left(\frac{\partial \mathbb{P}Q}{\partial x}, W\omega \right)_{\Omega^k} + \frac{1}{2} \langle Q^+ - \mathbb{P}Q, W\omega n_x \rangle_{\partial\Omega^k} + \frac{1}{2} \langle \mathcal{E}(Q), \mathbb{P}(W\omega) n_x \rangle_{\partial\Omega^k} \right], \end{aligned} \tag{2.9}$$

for all $\omega \in V_h$.

It was shown in [10] that this derivative operator D_h^x satisfies the global analogue of IBP property

$$(D_h^x Q, W\omega)_\Omega = - (Q, D_h^x(W\omega))_\Omega + \langle Q n_x, W\omega \rangle_{\partial\Omega}, \tag{2.10}$$

for $Q \in H^1(\Omega_h)$ and $W \in V_h$. If $W\omega = 1$, we have

$$(D_h^x Q, 1)_\Omega = \langle Q, n_x \rangle_{\partial\Omega}, \tag{2.11}$$

since $(Q, D_h^x 1)_\Omega = 0$. The entropy conservative DG formulation on the entire computational domain involving multiple elements is given by: find $Q \in V_h$, such that

$$\left(\frac{\partial Q}{\partial t}, \omega \right)_\Omega + \left((2D_h^x \mathbf{f}_S(\mathbf{Q}_e(x), \mathbf{Q}_e(y)))|_{y=x}, \omega \right)_\Omega = 0, \tag{2.12}$$

holds for all the test functions $\omega \in V_h$, where $\mathbf{Q}_e(x)$ is defined as $\mathbf{Q}(\mathbb{P}\mathbf{e}(x))$. In general, the boundary terms appearing in D_h^x term [following the definition in (2.9)] interact with volume terms, which can be simplified for diagonal norm SBP operators with boundary nodes.

The entropy conservation property of this method is provided in the following theorem:

Theorem 1 *By assuming that the numerical flux function f_S admits an absolutely convergent expansion [10], the DG methods on multiple elements (2.12) are globally entropy conservative in the sense that*

$$\left(\frac{\partial U(\mathbf{Q})}{\partial t}, 1 \right)_{\Omega} = \langle \psi, 1n_x \rangle_{\partial\Omega} - \langle \mathbf{f}(\mathbf{Q}_e), (\mathbb{P}\mathbf{e})n_x \rangle_{\partial\Omega}. \tag{2.13}$$

An equivalent form of the DG methods (2.12), which uses the vector variables and local matrices to guide the implementation, is available in [9].

3 Entropy Stable DG Method for the One-Dimensional SWEs

In this section, we extend the entropy conservative DG methods [9] to the one-dimensional SWEs with a non-zero source term representing the effect of a non-flat bottom topography. By carefully discretizing the source term and adding a positivity-preserving limiter, we will show that the resulting DG methods satisfy the properties of entropy stable, well-balanced and positivity-preserving at the same time.

The one-dimensional SWEs with a non-flat bottom take the form of

$$\frac{\partial \mathbf{Q}}{\partial t} + \frac{\partial \mathbf{f}(\mathbf{Q})}{\partial x} = \mathbf{S}(b, \mathbf{Q}), \tag{3.1}$$

with the conservation variables, the flux and source terms given by

$$\mathbf{Q} = \begin{bmatrix} h \\ hu \end{bmatrix}, \quad \mathbf{f} = \begin{bmatrix} hu \\ hu^2 + \frac{1}{2}gh^2 \end{bmatrix}, \quad \mathbf{S} = \begin{bmatrix} 0 \\ -ghb_x \end{bmatrix},$$

where $h(x, t)$ is the water height, $u(x, t)$ is the velocity, $m = hu$ is the momentum, $b(x, t)$ is the bottom topography, g is the gravitational constant. The entropy variables of the SWEs with the non-flat bottom are

$$\mathbf{e} = \begin{bmatrix} e_1 \\ e_2 \end{bmatrix} = \begin{bmatrix} g(h + b) - \frac{1}{2}u^2 \\ u \end{bmatrix}, \tag{3.2}$$

with the entropy U and the entropy potential ψ taking the form of

$$U = \frac{1}{2}hu^2 + \frac{1}{2}gh^2 + ghb, \quad \psi = \frac{1}{2}gh^2u. \tag{3.3}$$

3.1 Entropy Conservative DG Methods for the SWEs

We start by presenting the entropy conservative DG methods for the one-dimensional SWEs with a non-flat bottom. The main idea follows the setup of the entropy conservative methods in [10] (summarized in Sect. 2), with extra attention paid to the discretization of the new added source term to ensure that it won't affect the entropy conservation property and at the same time achieves the well-balanced property.

The same weak derivative operator D_h^x defined in Definition 3 is adopted to derive the entropy conservative DG methods for the SWEs, which take the form of

$$\left(\frac{\partial \mathbf{Q}}{\partial t}, \omega \right)_{\Omega} + \left((2D_h^x \mathbf{f}_S(\mathbf{Q}_e(x), \mathbf{Q}_e(y)))|_{y=x}, \omega \right)_{\Omega} = \begin{pmatrix} 0 \\ (-gh_e D_h^x b_e, \omega)_{\Omega} \end{pmatrix}, \tag{3.4}$$

where

$$\mathbf{Q}_e = \mathbf{Q}(\mathbb{P}e) = \begin{bmatrix} h_e \\ m_e \end{bmatrix}, \quad h_e = \frac{1}{g} \left(\mathbb{P}e_1 + \frac{1}{2} (\mathbb{P}e_2)^2 - g\mathbb{P}b \right), \quad m_e = h_e \mathbb{P}e_2, \quad b_e = \mathbb{P}b. \tag{3.5}$$

The entropy conservative fluxes \mathbf{f}_S for the one-dimensional SWEs with a non-flat bottom topography [19] are defined as follows.

Definition 4 Let $\mathbf{f}_S(\mathbf{Q}_l, \mathbf{Q}_r)$ be a consistent and symmetric numerical flux. It is entropy conservative for the shallow water system (3.1) if

$$(\mathbf{e}_l - \mathbf{e}_r)^T \mathbf{f}_S(\mathbf{Q}_l, \mathbf{Q}_r) = (\psi_l - \psi_r) + \frac{1}{2}g(b_l - b_r)(m_l + m_r), \tag{3.6}$$

holds for the entropy variables $\mathbf{e}_j = \mathbf{e}(\mathbf{Q}_j)$ and the scalar entropy potential $\psi_j = \psi(\mathbf{e}(\mathbf{Q}_j))$, $j = l, r$.

For the SWEs, the entropy conservative numerical flux \mathbf{f}_S [19] is given by

$$\mathbf{f}_S(\mathbf{Q}_l, \mathbf{Q}_r) = \begin{bmatrix} f_S^{(1)} \\ f_S^{(2)} \end{bmatrix} = \begin{bmatrix} \frac{1}{2}(m_l + m_r) \\ \frac{1}{4}(m_l + m_r)(u_l + u_r) + \frac{1}{2}gh_lh_r \end{bmatrix}. \tag{3.7}$$

By expanding the definition of the weak derivative operator D_h^x , and using the fact that $\mathbb{P}\omega = \omega$ when $\omega \in V_h$, the DG methods (3.4) can be expanded as

$$\begin{aligned} \sum_k \left(\frac{\partial h}{\partial t}, \omega \right)_{\Omega_k} + \left(\frac{\partial \mathbb{P}m_e}{\partial x}, \omega \right)_{\Omega_k} + \left\langle f_S^{(1)}(Q_e^+, Q_e) - \mathbb{P}m_e, \omega n_x \right\rangle_{\partial\Omega_k} &= 0, \\ \sum_k \left(\frac{\partial m}{\partial t}, \omega \right)_{\Omega_k} + (\text{I} + \text{II}, \omega)_{\Omega_k} + \left\langle f_S^{(2)}(Q_e^+, Q_e) - \text{III} - \text{IV}, \omega n_x \right\rangle_{\partial\Omega_k} + \text{V} + \text{VI} &= 0, \end{aligned} \tag{3.8}$$

with the terms I–VI defined by

$$\left\{ \begin{aligned} \text{I} &= \frac{1}{2} \left(\frac{\partial}{\partial x} (\mathbb{P}(m_e u_e)) + u_e \frac{\partial}{\partial x} (\mathbb{P}m_e) + m_e \frac{\partial}{\partial x} (u_e) \right), \\ \text{II} &= gh_e \frac{\partial}{\partial x} (\mathbb{P}h_e + b_e), \\ \text{III} &= \frac{1}{4} (2\mathbb{P}(m_e u_e) + (\mathbb{P}m_e)u_e + m_e u_e), \\ \text{IV} &= \frac{1}{2} gh_e (\mathbb{P}h_e - \llbracket b_e \rrbracket), \\ \text{V} &= \frac{1}{4} (\mathcal{E}(m_e), \mathbb{P}(u_e \omega) n_x)_{\partial\Omega_k}, \\ \text{VI} &= \frac{1}{2} g (\mathcal{E}(h_e), \mathbb{P}(h_e \omega) n_x)_{\partial\Omega_k}. \end{aligned} \right. \tag{3.9}$$

Remark 1 Although derived from different approaches, the resulting formulation is similar to the one in [11] (where a nodal DG discretization is used, and the bottom b is constant):

$$\frac{\partial hu}{\partial t} + \frac{1}{2} \frac{\partial hu^2}{\partial x} + \frac{1}{2} u \frac{\partial hu}{\partial x} + \frac{1}{2} hu \frac{\partial u}{\partial x} + gh \frac{\partial h}{\partial x} = 0, \tag{3.10}$$

and the skew-symmetric form in [22]:

$$\frac{1}{2} \left(\frac{\partial hu}{\partial t} + h \frac{\partial u}{\partial t} \right) + \frac{1}{2} \left(\frac{\partial hu^2}{\partial x} + hu \frac{\partial u}{\partial x} \right) + gh \frac{\partial h}{\partial x} = 0. \tag{3.11}$$

Next, we will show that the proposed DG method for the SWEs is semi-discretely entropy conservative.

Theorem 2 *For the global domain Ω , the DG methods (3.4) is globally entropy conservative in the sense that*

$$\left(\frac{\partial U(\mathbf{Q})}{\partial t}, 1 \right)_{\Omega} = \langle \psi, 1n_x \rangle_{\partial\Omega} - \langle \mathbf{f}(\mathbf{Q}_e), \mathbb{P}\mathbf{e}n_x \rangle_{\partial\Omega}. \tag{3.12}$$

Proof Taking $\mathbb{P}\mathbf{e}$ as test function (i.e., $\mathbb{P}e_1$ as the test function of the first equation, $\mathbb{P}e_2$ as the test function of the second equation, and summing the resulting two equations up), the DG method (3.4) becomes

$$\left(\frac{\partial \mathbf{Q}}{\partial t}, \mathbb{P}\mathbf{e} \right)_{\Omega} + \left((2D_h^x \mathbf{f}_S(\mathbf{Q}_e(x), \mathbf{Q}_e(y)))|_{y=x}, \mathbb{P}\mathbf{e} \right)_{\Omega} + (gh_e D_h^x b_e, \mathbb{P}e_2)_{\Omega} = 0, \tag{3.13}$$

and the first term yields

$$\left(\frac{\partial \mathbf{Q}}{\partial t}, \mathbb{P}\mathbf{e}(\mathbf{Q}) \right)_{\Omega} = \left(\frac{\partial \mathbf{Q}}{\partial t}, \mathbf{e}(\mathbf{Q}) \right)_{\Omega} = \left(\frac{\partial U(\mathbf{Q})}{\partial t}, 1 \right)_{\Omega}.$$

Following the definition, we can expand \mathbf{f}_S as

$$\begin{aligned} & \mathbf{f}_S(\mathbf{Q}(x), \mathbf{Q}(y)) \\ &= \left[\begin{array}{l} \frac{1}{2} (m(x) + m(y)) \\ \frac{1}{4} (m(x)u(x) + m(x)u(y) + m(y)u(x) + m(y)u(y)) + \frac{1}{2} gh(x)h(y) \end{array} \right] \\ &:= \left[\begin{array}{l} \sum_{i=1}^2 \zeta_i(x)\eta_i(y) \\ \sum_{i=3}^7 \zeta_i(x)\eta_i(y) \end{array} \right] = \sum_{i=1}^2 \left[\begin{array}{l} \zeta_i(\mathbf{Q}(x)) \\ 0 \end{array} \right] \eta_i(\mathbf{Q}(y)) + \sum_{i=3}^7 \left[\begin{array}{l} 0 \\ \zeta_i(\mathbf{Q}(x)) \end{array} \right] \eta_i(\mathbf{Q}(y)) \\ &:= \sum_{i=1}^7 \hat{\zeta}_i(\mathbf{Q}(x))\eta_i(\mathbf{Q}(y)), \end{aligned}$$

where, for the ease of presentation, we introduced the notations

$$(\zeta_1(\mathbf{Q}(x)), \zeta_2(\mathbf{Q}(x)), \dots, \zeta_7(\mathbf{Q}(x))) = (m(x), 1, m(x)u(x), m(x), u(x), 1, gh(x)),$$

and

$$(\eta_1(\mathbf{Q}(y)), \eta_2(\mathbf{Q}(y)), \dots, \eta_7(\mathbf{Q}(y))) = \frac{1}{4}(2, 2m(y), 1, u(y), m(y), m(y)u(y), 2h(y)).$$

Therefore, the second term of (3.13) becomes

$$\begin{aligned}
 \left((D_h^x \mathbf{f}_S(\mathbf{Q}_e(x), \mathbf{Q}_e(y)))|_{y=x}, \mathbb{P}\mathbf{e} \right)_\Omega &= \left(\left(D_h^x \sum_{i=1}^7 \hat{\zeta}_i(\mathbf{Q}_e(x)) \eta_i(\mathbf{Q}_e(y)) \right) \Big|_{y=x}, \mathbb{P}\mathbf{e}(x) \right)_\Omega \\
 &= \sum_{i=1}^7 \left(D_h^x \hat{\zeta}_i(\mathbf{Q}_e(x)), \eta_i(\mathbf{Q}_e(x)) \mathbb{P}\mathbf{e}(x) \right)_\Omega \\
 &= \sum_{i=1}^7 \left[- \left(\hat{\zeta}_i(\mathbf{Q}_e(x)), D_h^x (\eta_i(\mathbf{Q}_e(x)) \mathbb{P}\mathbf{e}(x)) \right)_\Omega + \left\langle \hat{\zeta}_i(\mathbf{Q}_e(x)) \eta_i(\mathbf{Q}_e(x)), \mathbb{P}\mathbf{e}(x) n_x \right\rangle_{\partial\Omega} \right] \\
 &= - \left((D_h^x (\mathbf{f}_S(\mathbf{Q}_e(y), \mathbf{Q}_e(x)) \cdot \mathbb{P}\mathbf{e}(x)))|_{y=x}, 1 \right)_\Omega + \left\langle \mathbf{f}_S(\mathbf{Q}_e(x), \mathbf{Q}_e(x)), \mathbb{P}\mathbf{e}(x) n_x \right\rangle_{\partial\Omega} \\
 &= - \left((D_h^x (\mathbf{f}_S(\mathbf{Q}_e(x), \mathbf{Q}_e(y)) \cdot \mathbb{P}\mathbf{e}(x)))|_{y=x}, 1 \right)_\Omega + \left\langle \mathbf{f}(\mathbf{Q}_e(x)), \mathbb{P}\mathbf{e}(x) n_x \right\rangle_{\partial\Omega}, \tag{3.14}
 \end{aligned}$$

where the third equality comes from the IBP property (2.10), and the last equality utilizes the symmetry and consistency of the entropy conservative flux \mathbf{f}_S . Note that

$$\left((D_h^x \mathbf{f}_S(\mathbf{Q}_e(x), \mathbf{Q}_e(y)))|_{y=x}, \mathbb{P}\mathbf{e}(x) \right)_\Omega = \left((D_h^x (\mathbf{f}_S(\mathbf{Q}_e(x), \mathbf{Q}_e(y)) \cdot \mathbb{P}\mathbf{e}(y)))|_{y=x}, 1 \right)_\Omega.$$

Combining this with (3.14), the flux term in the DG method (3.13) becomes

$$\begin{aligned}
 &\left((2D_h^x \mathbf{f}_S(\mathbf{Q}_e(x), \mathbf{Q}_e(y)))|_{y=x}, \mathbb{P}\mathbf{e} \right)_\Omega \\
 &= \left((D_h^x (\mathbf{f}_S(\mathbf{Q}_e(x), \mathbf{Q}_e(y)) \cdot (\mathbb{P}\mathbf{e}(y) - \mathbb{P}\mathbf{e}(x))))|_{y=x}, 1 \right)_\Omega + \left\langle \mathbf{f}(\mathbf{Q}_e(x)), \mathbb{P}\mathbf{e}(x) n_x \right\rangle_{\partial\Omega}. \tag{3.15}
 \end{aligned}$$

Using the fact that $\mathbf{e}(\mathbf{Q}(\mathbb{P}\mathbf{e})) = \mathbb{P}\mathbf{e}$, and the definition of entropy conservative flux \mathbf{f}_S in (3.6), we have

$$\begin{aligned}
 \mathbf{f}_S(\mathbf{Q}_e(x), \mathbf{Q}_e(y)) \cdot (\mathbb{P}\mathbf{e}(y) - \mathbb{P}\mathbf{e}(x)) &= \psi(y) - \psi(x) + \frac{1}{2} g(b_e(y) - b_e(x))(h_e(y)u_e(y) \\
 &\quad + h_e(x)u_e(x)),
 \end{aligned}$$

and the Eq. (3.15) becomes

$$\begin{aligned}
 &\left((2D_h^x \mathbf{f}_S(\mathbf{Q}_e(x), \mathbf{Q}_e(y)))|_{y=x}, \mathbb{P}\mathbf{e} \right)_\Omega \\
 &= \left(D_h^x \left(\psi(y) - \psi(x) + \frac{g}{2} (b_e(y) - b_e(x))(h_e(y)u_e(y) + h_e(x)u_e(x)) \right) \Big|_{y=x}, 1 \right)_\Omega \\
 &\quad + \left\langle \mathbf{f}(\mathbf{Q}_e), \mathbb{P}\mathbf{e} n_x \right\rangle_{\partial\Omega} \\
 &= \left\langle -\psi, 1 n_x \right\rangle_{\partial\Omega} + \left\langle \mathbf{f}(\mathbf{Q}_e), \mathbb{P}\mathbf{e} n_x \right\rangle_{\partial\Omega} + \frac{1}{2} g \left(D_h^x \left((b_e(y) - b_e(x))(h_e(y)\mathbb{P}e_2(y) \right. \right. \\
 &\quad \left. \left. + h_e(x)\mathbb{P}e_2(x)) \right) \Big|_{y=x}, 1 \right)_\Omega, \tag{3.16}
 \end{aligned}$$

where the last equality follows from the global IBP property in (2.11) and the replacement of u_e by $\mathbb{P}e_2$.

Next, we apply the IBP property (2.10) to the third term of Eq. (3.13) and obtain

$$\begin{aligned}
 & \left(h_e(x) D_h^x b_e(x), \mathbb{P}e_2(x) \right)_\Omega \\
 &= - \left(b_e(x), D_h^x (h_e(x) \mathbb{P}e_2(x)) \right)_\Omega + \left\langle b_e(x) h_e(x) \mathbb{P}e_2(x), n_x \right\rangle_{\partial\Omega} \\
 &= - \left(b_e(y)|_{y=x}, D_h^x (h_e(x) \mathbb{P}e_2(x)) \right)_\Omega + \left\langle b_e(x) h_e(x) \mathbb{P}e_2(x), n_x \right\rangle_{\partial\Omega} \\
 &= - \left(D_h^x (b_e(y) h_e(x) \mathbb{P}e_2(x)) \Big|_{y=x}, 1 \right)_\Omega + \left\langle b_e(x) h_e(x) \mathbb{P}e_2(x), n_x \right\rangle_{\partial\Omega}.
 \end{aligned} \tag{3.17}$$

Using again the fact that

$$\left(h_e(x) D_h^x b_e(x), \mathbb{P}e_2(x) \right)_\Omega = \left(D_h^x (b_e(x) h_e(y) \mathbb{P}e_2(y)) \Big|_{y=x}, 1 \right)_\Omega,$$

the source term (3.17) can be manipulated to yield

$$\begin{aligned}
 \left(h_e(x) D_h^x b_e(x), \mathbb{P}e_2(x) \right)_\Omega &= \frac{1}{2} \left(h_e(x) D_h^x b_e(x), \mathbb{P}e_2(x) \right)_\Omega + \frac{1}{2} \left(h_e(x) D_h^x b_e(x), \mathbb{P}e_2(x) \right)_\Omega \\
 &= \frac{1}{2} \left(D_h^x (b_e(x) h_e(y) \mathbb{P}e_2(y) - b_e(y) h_e(x) \mathbb{P}e_2(x)) \Big|_{y=x}, 1 \right)_\Omega + \frac{1}{2} \left\langle b_e(x) h_e(x) \mathbb{P}e_2(x), n_x \right\rangle_{\partial\Omega}.
 \end{aligned} \tag{3.18}$$

The sum of the flux term (3.16) and the source term (3.18) yields

$$\begin{aligned}
 & \left(2D_h^x \mathbf{f}_S(\mathbf{Q}_e(x), \mathbf{Q}_e(y)) \Big|_{y=x}, \mathbb{P}\mathbf{e} \right)_\Omega + \left(gh_e(x) D_h^x b_e(x), \mathbb{P}e_2(x) \right)_\Omega \\
 &= \left\langle -\psi, 1n_x \right\rangle_{\partial\Omega} + \left\langle \mathbf{f}(\mathbf{Q}_e), \mathbb{P}\mathbf{e}n_x \right\rangle_{\partial\Omega} \\
 &+ \frac{g}{2} \left(D_h^x \left((b_e(y) - b_e(x))(h_e(y) \mathbb{P}e_2(y) + h_e(x) \mathbb{P}e_2(x)) \right) \Big|_{y=x}, 1 \right)_\Omega \\
 &+ \frac{g}{2} \left(D_h^x (b_e(x) h_e(y) \mathbb{P}e_2(y) - b_e(y) h_e(x) \mathbb{P}e_2(x)) \Big|_{y=x}, 1 \right)_\Omega + \frac{g}{2} \left\langle b_e(x), h_e(x) \mathbb{P}e_2(x) n_x \right\rangle_{\partial\Omega} \\
 &= \left\langle -\psi, 1n_x \right\rangle_{\partial\Omega} + \left\langle \mathbf{f}(\mathbf{Q}_e), \mathbb{P}\mathbf{e}n_x \right\rangle_{\partial\Omega} + \frac{g}{2} \left(D_h^x (b_e(y) h_e(y) \mathbb{P}e_2(y) - b_e(x) h_e(x) \mathbb{P}e_2(x)) \Big|_{y=x}, 1 \right)_\Omega \\
 &+ \frac{g}{2} \left\langle b_e(x), h_e(x) \mathbb{P}e_2(x) n_x \right\rangle_{\partial\Omega} \\
 &= \left\langle -\psi, 1n_x \right\rangle_{\partial\Omega} + \left\langle \mathbf{f}(\mathbf{Q}_e), \mathbb{P}\mathbf{e}n_x \right\rangle_{\partial\Omega} \\
 &+ \frac{g}{2} \left[- \left(D_h^x (b_e(x) h_e(x) \mathbb{P}e_2(x)), 1 \right)_\Omega + \left\langle b_e(x), h_e(x) \mathbb{P}e_2(x) n_x \right\rangle_{\partial\Omega} \right] \\
 &= \left\langle -\psi, 1n_x \right\rangle_{\partial\Omega} + \left\langle \mathbf{f}(\mathbf{Q}_e), \mathbb{P}\mathbf{e}n_x \right\rangle_{\partial\Omega}.
 \end{aligned}$$

Combined with the Eq. (3.13), this leads to the entropy conservation property (3.12). □

3.2 Local Conservation Property

The entropy conservative DG methods (3.8) involve the approximation of the derivatives in the non-conservative form. As it is well-known from the Lax–Wendroff theorem, any numerical methods for the hyperbolic conservation laws should be in the conservative form to ensure that the solution will converge to the weak solution. In this subsection, we will demonstrate that the entropy conservative DG methods written in the form of (3.8) indeed have the local conservation property, which is summarized in the following theorem.

Theorem 3 *When the test function $\omega = 1$, the DG method (3.8) reduces to*

$$\begin{aligned} \left(\frac{\partial h}{\partial t}, 1\right)_{\Omega_k} + \langle f_S^{(1)}(\mathbf{Q}_e^+, \mathbf{Q}_e), n_x \rangle_{\partial\Omega_k} &= 0, \\ \left(\frac{\partial m}{\partial t}, 1\right)_{\Omega_k} + \langle f_S^{(2)}(\mathbf{Q}_e^+, \mathbf{Q}_e), n_x \rangle_{\partial\Omega_k} &= - \left(gh_e \frac{\partial}{\partial x} b_e, 1\right)_{\Omega_k} - \left\langle \frac{1}{2}gh_e \llbracket b_e \rrbracket, n_x \right\rangle_{\partial\Omega_k}. \end{aligned} \tag{3.19}$$

When the bottom topography b is flat, it becomes

$$\left(\frac{\partial \mathbf{Q}}{\partial t}, 1\right)_{\Omega^k} + \langle f_S(\mathbf{Q}_e^+, \mathbf{Q}_e), n_x \rangle_{\partial\Omega^k} = 0.$$

This means our method is locally conservative, similar as the conventional DG methods for the SWEs.

Proof By taking the test function $\omega = 1$ in the element Ω_k and $\omega = 0$ everywhere else, the DG method (3.8) reduces to

$$\left(\frac{\partial h}{\partial t}, 1\right)_{\Omega_k} + \left(\frac{\partial \mathbb{P}m_e}{\partial x}, 1\right)_{\Omega_k} + \langle f_S^{(1)}(\mathbf{Q}_e^+, \mathbf{Q}_e) - \mathbb{P}m_e, n_x \rangle_{\partial\Omega_k} = 0, \tag{3.20}$$

$$\left(\frac{\partial m}{\partial t}, 1\right)_{\Omega_k} + (\text{I} + \text{II}, 1)_{\Omega_k} + \langle f_S^{(2)}(\mathbf{Q}_e^+, \mathbf{Q}_e) - \text{III} - \text{IV}, n_x \rangle_{\partial\Omega_k} + \text{V} + \text{VI} = 0, \tag{3.21}$$

with the terms I–IV defined in (3.9), and

$$\text{V} = \frac{1}{4} \langle \mathcal{E}(m_e) \mathbb{P}u_e, n_x \rangle_{\partial\Omega_k}, \quad \text{VI} = \frac{1}{2} g \langle \mathcal{E}(h_e) \mathbb{P}h_e, n_x \rangle_{\partial\Omega_k}. \tag{3.22}$$

It is easy to observe that

$$\left(\frac{\partial \mathbb{P}m_e}{\partial x}, 1\right)_{\Omega^k} = \langle \mathbb{P}m_e, n_x \rangle_{\partial\Omega^k},$$

therefore, the first Eq. (3.20) reduces to

$$\left(\frac{\partial h}{\partial t}, 1\right)_{\Omega_k} + \langle f_S^{(1)}(\mathbf{Q}_e^+, \mathbf{Q}_e), n_x \rangle_{\partial\Omega_k} = 0.$$

To simplify the second Eq. (3.21), we first notice that $u_e = m_e/h_e = \mathbb{P}e_2 \in V_h$, following the definition of \mathbf{Q}_e in (3.5), therefore, $\mathbb{P}(u_e) = u_e$. By utilizing the following equalities

$$\begin{aligned} \left(\frac{\partial}{\partial x} \mathbb{P}(m_e u_e), 1\right)_{\Omega^k} &= \langle \mathbb{P}(m_e u_e), n_x \rangle_{\partial\Omega^k}, \\ \left(u_e \frac{\partial}{\partial x} \mathbb{P}m_e + m_e \frac{\partial}{\partial x} u_e, 1\right)_{\Omega^k} &= \left(u_e \frac{\partial}{\partial x} \mathbb{P}m_e + (\mathbb{P}m_e) \frac{\partial}{\partial x} u_e, 1\right)_{\Omega^k} = \langle \mathbb{P}m_e u_e, n_x \rangle_{\partial\Omega^k}, \\ \left(h_e \frac{\partial}{\partial x} \mathbb{P}h_e, 1\right)_{\Omega^k} &= \left(\mathbb{P}h_e \frac{\partial}{\partial x} \mathbb{P}h_e, 1\right)_{\Omega^k} = \left\langle \frac{1}{2} \mathbb{P}h_e \mathbb{P}h_e, n_x \right\rangle_{\partial\Omega^k}, \end{aligned}$$

we can show that

$$\begin{aligned}
 & (I, 1)_{\Omega^k} - \langle III, n_x \rangle_{\partial\Omega^k} + V \\
 &= \frac{1}{2} \langle \mathbb{P}(m_e u_e), n_x \rangle_{\partial\Omega^k} + \frac{1}{2} \langle (\mathbb{P}m_e) u_e, n_x \rangle_{\partial\Omega^k} \\
 & \quad - \left\langle \frac{1}{2} \mathbb{P}(m_e u_e) + \frac{1}{4} (\mathbb{P}m_e) u_e + \frac{1}{4} m_e u_e, n_x \right\rangle_{\partial\Omega^k} + \frac{1}{4} \langle \mathcal{E}(m_e), (\mathbb{P}u_e) n_x \rangle_{\partial\Omega^k} \\
 &= \frac{1}{2} \langle \mathbb{P}m_e u_e, n_x \rangle_{\partial\Omega^k} - \frac{1}{4} \langle (\mathbb{P}m_e) u_e + m_e u_e, n_x \rangle_{\partial\Omega^k} + \frac{1}{4} \langle m_e - \mathbb{P}m_e, u_e n_x \rangle_{\partial\Omega^k} = 0,
 \end{aligned}$$

and

$$\begin{aligned}
 & (II, 1)_{\Omega^k} - \langle IV, n_x \rangle_{\partial\Omega^k} + VI \\
 &= \left(gh_e \frac{\partial}{\partial x} \mathbb{P}h_e + gh_e \frac{\partial}{\partial x} b_e, 1 \right)_{\Omega_k} \\
 & \quad - \frac{g}{2} \left(\langle h_e \mathbb{P}h_e - h_e \llbracket b_e \rrbracket, n_x \rangle_{\partial\Omega^k} - \langle h_e - \mathbb{P}h_e, (\mathbb{P}h_e) n_x \rangle_{\partial\Omega^k} \right) \\
 &= \left(gh_e \frac{\partial}{\partial x} b_e, 1 \right)_{\Omega_k} + \left\langle \frac{1}{2} gh_e \llbracket b_e \rrbracket, n_x \right\rangle_{\partial\Omega^k}.
 \end{aligned}$$

Therefore, the second Eq. (3.21) reduces to

$$\left(\frac{\partial m}{\partial t}, 1 \right)_{\Omega_k} + \left\langle f_S^{(2)}(\mathbf{Q}_e^+, \mathbf{Q}_e), n_x \right\rangle_{\partial\Omega_k} = - \left(gh_e \frac{\partial}{\partial x} b_e, 1 \right)_{\Omega_k} - \left\langle \frac{1}{2} gh_e \llbracket b_e \rrbracket, n_x \right\rangle_{\partial\Omega^k},$$

which completes our proof. □

3.3 Entropy Stable Scheme

The proposed DG method (3.8) is shown to be entropy conservative, which is desirable for smooth solutions. However, for the numerical solutions of the hyperbolic balance laws which may develop discontinuity, entropy stable methods are usually preferred when the discontinuity appears in the solution. In this subsection, we present how to obtain the entropy stable DG methods for the SWEs and provide the analytical proof of it.

Following the idea of the Lax–Friedrichs numerical flux, we could add additional dissipative terms at the element interfaces, and construct the entropy stable DG methods in the form of

$$\begin{aligned}
 & \left(\frac{\partial \mathbf{Q}}{\partial t}, \omega \right)_{\Omega} + \left((2D_h^x \mathbf{f}_S(\mathbf{Q}_e(x), \mathbf{Q}_e(y)))|_{y=x}, \omega \right)_{\Omega} \\
 & \quad - \sum_k \frac{\alpha}{2} \langle \llbracket \mathbf{M} \rrbracket, \omega n_x \rangle_{\partial\Omega^k} = \left(\begin{matrix} 0 \\ -gh_e D_h^x b_e \end{matrix}, \omega \right)_{\Omega}, \tag{3.23}
 \end{aligned}$$

where $\alpha = \max(|u| + \sqrt{gh})$ denotes the maximum eigenvalue of the Jacobian matrix of the flux. The extra term $-\sum_k \frac{\alpha}{2} \langle \llbracket \mathbf{M} \rrbracket, \omega n_x \rangle_{\partial\Omega^k}$, with $\mathbf{M} = \begin{pmatrix} h_e + b_e \\ (h_e + b_e)u_e \end{pmatrix}$, represents additional numerical dissipation. Note that $\langle \llbracket h_e + b_e \rrbracket, \omega n_x \rangle_{\partial\Omega^k}$, which reduces to $\langle \llbracket h_e \rrbracket, \omega n_x \rangle_{\partial\Omega^k}$ when the bottom function $b_e = 0$, is used for the purpose of well-balanced property to be explained in the next subsection. The proof of the entropy stable property is provided below.

Theorem 4 *The DG method (3.23) is semi-discretely entropy stable in the sense that*

$$\left(\frac{\partial U(\mathbf{Q})}{\partial t}, 1 \right)_{\Omega} \leq \langle \psi, 1n_x \rangle_{\partial\Omega} - \langle \mathbf{f}(\mathbf{Q}_e), \mathbb{P}e_n \rangle_{\partial\Omega}. \tag{3.24}$$

Proof By taking the test function $\omega = \mathbb{P}e$ in (3.23), and following the same steps in the proof of the entropy conservative property, we can obtain

$$\begin{aligned} \left(\frac{\partial U(\mathbf{Q})}{\partial t}, 1 \right)_{\Omega} &= \langle \psi, 1n_x \rangle_{\partial\Omega} + \langle \mathbf{f}(\mathbf{Q}_e), \mathbb{P}e_n \rangle_{\partial\Omega} + \frac{\alpha}{2} \sum_k \langle [\mathbf{M}], \mathbb{P}e_n \rangle_{\partial\Omega^k} \\ &= \langle \psi, 1n_x \rangle_{\partial\Omega} + \langle \mathbf{f}(\mathbf{Q}_e), \mathbb{P}e_n \rangle_{\partial\Omega} - \frac{\alpha}{2} \sum_k [\mathbf{M}]|_{x_{k+\frac{1}{2}}} [\mathbb{P}e]|_{x_{k+\frac{1}{2}}}. \end{aligned} \tag{3.25}$$

For simplicity, let us denote $\mathbb{P}e = [\hat{e}_1, \hat{e}_2]^T$. From the definition (3.5), we have $h_e + b_e = \frac{1}{g}(\hat{e}_1 + \frac{1}{2}\hat{e}_2^2)$ and $u_e = \hat{e}_2$. Using the equality that

$$[[ab]] = [[a]]\{b\} + \{a\}[[b]],$$

where $[[\cdot]]$ and $\{\cdot\}$ stand for the jump and cell average, the last term of Eq. (3.25) at the interface $x_{k+1/2}$ (this subindex is ignored in the following formula) satisfies

$$\begin{aligned} - \left(\frac{[[h_e + b_e]]}{[[h_e + b_e]u_e]} \right) [\mathbb{P}e] &= \begin{bmatrix} (h_e + b_e)^+ - (h_e + b_e) \\ (m_e)^+ - m_e \end{bmatrix} \cdot \begin{bmatrix} \hat{e}_1 - \hat{e}_1^+ \\ \hat{e}_2 - \hat{e}_2^+ \end{bmatrix} \\ &= -\frac{1}{g} \left([[\hat{e}_1]][\hat{e}_1] + \frac{1}{2}[[\hat{e}_2^2]][\hat{e}_1] + [[\hat{e}_1\hat{e}_2]][\hat{e}_2] + \frac{1}{2}[[\hat{e}_2^3]][\hat{e}_2] \right) \\ &= -\frac{1}{g} \left([[\hat{e}_1]]^2 + \{\hat{e}_2\}[[\hat{e}_2]][\hat{e}_1] + [[\hat{e}_1]]\{\hat{e}_2\}[[\hat{e}_2]] + \{\hat{e}_1\}[[\hat{e}_2]]^2 + \{\hat{e}_2\}^2[[\hat{e}_2]]^2 + \frac{1}{2}\{\hat{e}_2^2\}[[\hat{e}_2]]^2 \right) \\ &= -\frac{1}{g} \left(([[\hat{e}_1]] + \{\hat{e}_2\}[[\hat{e}_2]])^2 + \{\hat{e}_1 + \frac{1}{2}\hat{e}_2^2\}[[\hat{e}_2]]^2 \right) \\ &= -\frac{1}{g} \left(([[\hat{e}_1]] + \{\hat{e}_2\}[[\hat{e}_2]])^2 + g\{h_e + b_e\}[[\hat{e}_2]]^2 \right) \\ &\leq 0, \end{aligned}$$

where the last inequality follows from the fact that $h_e + b_e$ stays non-negative (see the positivity-preserving proof in Sect. 3.5). Therefore, the last term of (3.25) should always stay non-positive, and this leads to the entropy stable property (3.24). \square

Remark 2 As in Theorem 3, one can easily observe that the entropy stable scheme (3.23) is also locally conservative, after replacing $f_S^{(1)}(\mathbf{Q}_e^+, \mathbf{Q}_e)$ by $f_S^{(1)}(\mathbf{Q}_e^+, \mathbf{Q}_e) - \frac{\alpha}{2}[\mathbf{M}]$ in (3.19).

A slope limiter procedure is usually needed in the DG methods when the solution contains discontinuities. In this paper, we use the characteristic-wise total variation bounded (TVB) limiter in [15], with a corrected minmod function [14] defined by

$$\hat{m}(a_1, \dots, a_n) = \begin{cases} a_1, & \text{if } |a_1| \leq M\Delta x^2, \\ m(a_1, \dots, a_n), & \text{otherwise,} \end{cases} \tag{3.26}$$

where M is the TVB parameter, and the minmod function m is given by

$$m(a_1, \dots, a_n) = \begin{cases} s \min_i |a_i|, & \text{if } s = \text{sign}(a_1) = \dots = \text{sign}(a_n), \\ 0, & \text{otherwise.} \end{cases} \tag{3.27}$$

For the purpose of well-balanced, the slope limiter is applied on the variable $(h + b, m)^T$. We refer to [11] for the discussion on the compatibility of the entropy stable property and the TVD/TVB limiter.

3.4 Well-Balanced Property

Another desirable property of numerical methods for the SWEs is the well-balanced property for the still water steady state solution (1.2). Below, we will show that, with the proposed source term discretization, our entropy stable methods are well-balanced.

Theorem 5 *The entropy conservative DG method (3.8) and the entropy stable DG method (3.23) are both well-balanced for the still-water steady state solution, denoted by*

$$u = 0 \text{ and } h + b = \text{constant } C. \tag{3.28}$$

Proof Suppose the initial condition is at the still-water steady state (3.28), therefore, $h + b = C$ and $u = 0$. This leads to the entropy variable $\mathbf{e} = (gC, 0)^T$, hence $h_e = h$ and $(h_e + b_e)u_e = 0$ following the definition of \mathbf{Q}_e in (3.5). Below we will present the proof of well-balanced property of the entropy conservative method (3.8) only, and that of the entropy stable method follows directly, as the added viscosity term disappears at the steady state.

Using the fact that $(h_e + b_e)u_e = 0$, it is easy to observe that the first equation of the DG method (3.8) is well-balanced, and the second equation becomes

$$\begin{aligned} & \sum_k \left(\frac{\partial m}{\partial t}, \omega \right)_{\Omega_k} + \left(gh_e \frac{\partial}{\partial x} (\mathbb{P}h_e + b_e), \omega \right)_{\Omega_k} \\ & + \left\langle \frac{1}{2}gh_e h_e^+ - \frac{1}{2}gh_e \mathbb{P}h_e + \frac{1}{2}gh_e \llbracket b_e \rrbracket, \omega n_x \right\rangle_{\partial\Omega_k} + \frac{1}{2}g \langle h_e - \mathbb{P}h_e, \mathbb{P}(h_e \omega) n_x \rangle_{\partial\Omega_k} = 0. \end{aligned} \tag{3.29}$$

Since $h_e = h \in V_h, b_e = b \in V_h$, we have $\mathbb{P}h_e = h, \mathbb{P}b_e = b$, and $h_e + b_e = C$, hence $\llbracket h_e + b_e \rrbracket = 0$. Therefore,

$$\sum_k \left(\frac{\partial m}{\partial t}, \omega \right)_{\Omega_k} = 0,$$

holds exactly in the discrete level, and the well-balanced property is obtained. □

3.5 Positivity-Preservation Limiter

In this section, the positivity-preserving limiter in [43] will be incorporated into the proposed entropy stable, well-balanced DG methods, and we will show that this will not affect the entropy stable property.

To ensure the positivity-preserving property, we propose with the following modification of the well-balanced and entropy stable methods (3.23), by introducing the updated numerical fluxes at the cell interface. We first define

$$h_e^* = \max(h_e, 0), \quad m_e^* = h_e^* \frac{m_e}{h_e}, \tag{3.30}$$

at the cell interface, which gives us Q_e^* , as well as $Q_e^{*,+}$, at every cell interface $\partial\Omega_k$. Note that the updated cell interface values Q_e^* share similar formulation of the hydrostatic recon-

struction

$$h^* = \max(h + b - \max(b, b^+), 0),$$

which was employed in [43] to obtain positivity-preserving and well-balanced DG methods for the SWEs. The updated numerical methods take the form of

$$\begin{aligned} \sum_k \left(\frac{\partial h}{\partial t}, \omega \right)_{\Omega_k} + \left(\frac{\partial \mathbb{P}m_e}{\partial x}, \omega \right)_{\Omega_k} + \left\langle f_S^{(1)}(Q_e^{*,+}, Q_e^*) - \frac{\alpha}{2} \llbracket h_e^* + b_e \rrbracket - \mathbb{P}m_e, \omega n_x \right\rangle_{\partial\Omega_k} &= 0, \\ \sum_k \left(\frac{\partial m}{\partial t}, \omega \right)_{\Omega_k} + (\text{I} + \text{II}, \omega)_{\Omega_k} + \left\langle f_S^{(2)}(Q_e^+, Q_e) - \frac{\alpha}{2} \llbracket (h_e + b_e)u_e \rrbracket - \text{III} - \text{IV}, \omega n_x \right\rangle_{\partial\Omega_k} \\ + \text{V} + \text{VI} &= 0, \end{aligned} \tag{3.31}$$

with the same terms I–VI defined in (3.9).

As outlined in [43,46], the key components to achieve the positivity-preserving property are two items: the positivity of the proposed methods in the first order version, and a simple positivity-preserving limiter. For simplicity, we only consider the simple forward Euler time discretization, and the same results can be generalized to total variation diminishing (TVD) high order Runge–Kutta methods as shown in [43,46].

Take the test function to be $v = 1$ in the entropy stable methods (3.23). The first order version of the resulting equation for the cell average of the water height is given by

$$\bar{h}_k^{n+1} = \bar{h}_k^n - \lambda \left(\widehat{f}_S^{(1)}((Q_e^*)_{k+1}^n, (Q_e^*)_k^n) - \widehat{f}_S^{(1)}((Q_e^*)_{k-1}^n, (Q_e^*)_k^n) \right), \tag{3.32}$$

where n refers to the time step, $\lambda = \frac{\Delta t}{\Delta x}$ is the ratio of time and space mesh size and

$$\begin{aligned} \widehat{f}_S^{(1)}((Q_e^*)_{k+1}^n, (Q_e^*)_k^n) &= f_S^{(1)}((Q_e^*)_{k+1}^n, (Q_e^*)_k^n) - \frac{\alpha}{2} ((h_e^*)_{k+1}^n - (h_e^*)_k^n) \\ &= \frac{1}{2} ((m_e^*)_{k+1}^n + (m_e^*)_k^n - \alpha((h_e^*)_{k+1}^n - (h_e^*)_k^n)), \end{aligned}$$

is the numerical flux, which is very similar to the standard Lax–Friedrichs flux (with h, m replaced by h_e and m_e). Easy to observe the following positivity-preserving property of this first order method.

Lemma 1 *Under a standard CFL condition $\lambda\alpha \leq \min_k \left(\frac{h_k^n}{(h_e^*)_k^n} \right)$ with $\alpha = \max(|u_e| + \sqrt{gh_e})$, the scheme (3.32) is positivity-preserving in the sense that if the numerical solution \bar{h}_k^n is non-negative then the update solution \bar{h}_k^{n+1} is also non-negative.*

Proof The scheme (3.32) can be written as

$$\begin{aligned} h_k^{n+1} &= h_k^n - \lambda\alpha(h_e^*)_k^n + \frac{1}{2}\lambda(\alpha - u_{k+1}^n)(h_e^*)_{k+1}^n + \frac{1}{2}\lambda(\alpha + u_{k-1}^n)(h_e^*)_{k-1}^n \\ &= \left(\frac{h_k^n}{(h_e^*)_k^n} - \lambda\alpha \right) (h_e^*)_k^n + \frac{1}{2}\lambda(\alpha - u_{k+1}^n)(h_e^*)_{k+1}^n + \frac{1}{2}\lambda(\alpha + u_{k-1}^n)(h_e^*)_{k-1}^n. \end{aligned} \tag{3.33}$$

Here, h_k^{n+1} is a linear combination of $(h_e^*)_k^n$, $(h_e^*)_{k-1}^n$ and $(h_e^*)_{k+1}^n$ with non-negative coefficients. Thus, h_k^{n+1} is non-negative. □

For the high order entropy stable DG method (3.8), we have shown in Theorem 3 that

$$\left(\frac{\partial h}{\partial t}, 1 \right)_{\Omega^k} + \left\langle f_S^{(1)}(Q_e^{*,+}, Q_e^*), 1n_x \right\rangle_{\partial\Omega^k} = 0,$$

The main step to show the positivity-preserving property of this method is listed below, and we refer to [43] for the details. We introduce the M -point (with $2M - 3 \geq N$) Legendre Gauss–Lobatto quadrature rule (for the proof of positivity-preserving only, and not used in the implementation) on the interval I_j , and denote these quadrature points by $S_k = \left\{ x_{k-\frac{1}{2}} = \hat{x}_k^1, \hat{x}_k^2, \dots, \hat{x}_k^{M-1}, \hat{x}_k^M = x_{k+\frac{1}{2}} \right\}$, with the corresponding quadrature weights \hat{w}_r for the interval $[-1/2, 1/2]$ satisfying $\sum_{r=1}^M \hat{w}_r = 1$. It can be shown that if the numerical solution $h_k^n(x)$ is non-negative on these quadrature points S_k , then the update solution \bar{h}_k^{n+1} is also non-negative under the suitable CFL condition

$$\lambda\alpha \leq \hat{w}_1 \min_k \left(\frac{h_{k+1/2}^\pm}{(h_e^*)_{k+1/2}^\pm} \right). \tag{3.34}$$

The following positivity-preserving limiter [43,46] is then applied on the DG polynomial $\mathbf{Q}_j^n(x) = (h_k^n(x), m_j^n(x))^T$,

$$\tilde{\mathbf{Q}}_k^n(x) = \theta \left(\mathbf{Q}_k^n(x) - \bar{\mathbf{Q}}_k^n \right) + \bar{\mathbf{Q}}_k^n, \quad \theta = \min \left\{ 1, \frac{\bar{h}_k^n}{\bar{h}_k^n - d_k} \right\}, \tag{3.35}$$

with

$$d_k = \min_{x \in S_k} h_k^n(x) = \min_{r=1, \dots, M} h_k^n(\hat{x}_k^r). \tag{3.36}$$

With this choice of d_k , we can show that $\tilde{h}_k^n(\hat{x}_k^r) \geq 0$ ($r = 1, \dots, N$), and this limiter maintains the local conservation of the variable $\mathbf{Q}_k^n(x)$. The modified polynomial $\tilde{\mathbf{Q}}_j^n(x)$, instead of $\mathbf{Q}_j^n(x)$, is then used in the entropy stable methods (3.31). Following the proofs in [43,46], we can verify that the entropy stable methods coupled with this positivity-preserving limiter are high order accurate, positivity-preserving and mass conservation under the CFL condition (3.34). For the DG method, the CFL condition (3.34) is comparable with the standard linear stability CFL condition, but if one wants to take larger time step, we could implement the time step restriction (3.34) only when a preliminary calculation of the water height at the next time step has negative cell average.

Next, we show that this limiter won't affect the entropy stable property. Similar result has also been available in [11], as well as in [30,36].

Theorem 6 *The entropy stable method (3.31) is compatible with the positivity-preserving limiter (3.35).*

Proof For any convex entropy function U , we have

$$\begin{aligned} \overline{U(\tilde{\mathbf{Q}}_k)} &= \overline{U(\theta \mathbf{Q}_k + (1 - \theta) \bar{\mathbf{Q}}_k)} = \overline{\theta U(\mathbf{Q}_k) + (1 - \theta) U(\bar{\mathbf{Q}}_k)} \\ &\leq \theta \overline{U(\mathbf{Q}_k)} + (1 - \theta) \overline{U(\bar{\mathbf{Q}}_k)} \quad (\text{since } U \text{ is convex}) = \theta \overline{U(\mathbf{Q}_k)} + (1 - \theta) U(\bar{\mathbf{Q}}_k) \\ &\leq \theta \overline{U(\mathbf{Q}_k)} + (1 - \theta) \overline{U(\bar{\mathbf{Q}}_k)} \quad (\text{via Jensen's inequality}) = \overline{U(\bar{\mathbf{Q}}_k)}. \end{aligned}$$

Therefore, the modified polynomial $\tilde{\mathbf{Q}}$ has a entropy which is less than or equal to the original entropy, and we can conclude that the positivity-preserving limiter does not increase the entropy of the system. □

4 Entropy Stable DG Method for the Two-Dimensional SWEs

The one-dimensional entropy stable, well-balanced DG methods can be easily extended to two dimensions, which will be explained in this section. The two-dimensional SWEs with a non-flat bottom topography take the form of

$$\frac{\partial \mathbf{Q}}{\partial t} + \frac{\partial \mathbf{f}(\mathbf{Q})}{\partial x} + \frac{\partial \mathbf{g}(\mathbf{Q})}{\partial y} = \mathbf{S}, \tag{4.1}$$

with the conservative variables

$$\mathbf{Q} = \begin{bmatrix} h \\ m_1 \\ m_2 \end{bmatrix} = \begin{bmatrix} h \\ hu \\ hv \end{bmatrix},$$

the fluxes and source terms given by

$$\mathbf{f} = \begin{bmatrix} hu \\ hu^2 + \frac{1}{2}gh^2 \\ hvu \end{bmatrix}, \quad \mathbf{g} = \begin{bmatrix} hv \\ huv \\ hv^2 + \frac{1}{2}gh^2 \end{bmatrix}, \quad \mathbf{S} = \begin{bmatrix} 0 \\ -ghb_x \\ -ghb_y \end{bmatrix}.$$

The two-dimensional entropy variables are

$$\mathbf{e} = \begin{bmatrix} e_1 \\ e_2 \\ e_3 \end{bmatrix} = \begin{bmatrix} g(h + b) - \frac{1}{2}u^2 - \frac{1}{2}v^2 \\ u \\ v \end{bmatrix},$$

and the corresponding entropy, entropy potentials are

$$U = \frac{1}{2}h(u^2 + v^2) + \frac{1}{2}gh^2 + ghb, \quad \psi_1 = \frac{1}{2}gh^2u, \quad \psi_2 = \frac{1}{2}gh^2v.$$

The two-dimensional symmetric and consistent entropy conservative numerical fluxes $\mathbf{f}_S(\mathbf{Q}_l, \mathbf{Q}_r)$ and $\mathbf{g}_S(\mathbf{Q}_b, \mathbf{Q}_t)$, which satisfy the following definition

$$\begin{aligned} (\mathbf{e}_l - \mathbf{e}_r)^T \mathbf{f}_S(\mathbf{Q}_l, \mathbf{Q}_r) &= (\psi_{1,l} - \psi_{1,r}) + \frac{g}{2}(b_l - b_r)(m_{1,l} + m_{1,r}), \\ (\mathbf{e}_b - \mathbf{e}_t)^T \mathbf{g}_S(\mathbf{Q}_b, \mathbf{Q}_t) &= (\psi_{2,b} - \psi_{2,t}) + \frac{g}{2}(b_b - b_t)(m_{2,b} + m_{2,t}), \end{aligned} \tag{4.2}$$

have been studied [11] and are given by

$$\mathbf{f}_S(\mathbf{Q}_l, \mathbf{Q}_r) = \begin{bmatrix} f_S^{(1)} \\ f_S^{(2)} \\ f_S^{(3)} \end{bmatrix} = \begin{bmatrix} \frac{1}{2}(m_{1,l} + m_{1,r}) \\ \frac{1}{4}(m_{1,l} + m_{1,r})(u_l + u_r) + \frac{1}{2}gh_lh_r \\ \frac{1}{4}(m_{2,l} + m_{2,r})(u_l + u_r) \end{bmatrix}, \tag{4.3}$$

$$\mathbf{g}_S(\mathbf{Q}_b, \mathbf{Q}_t) = \begin{bmatrix} g_S^{(1)} \\ g_S^{(2)} \\ g_S^{(3)} \end{bmatrix} = \begin{bmatrix} \frac{1}{2} (m_{2,b} + m_{2,t}) \\ \frac{1}{4} (m_{1,b} + m_{1,t}) (v_b + v_t) \\ \frac{1}{4} (m_{2,b} + m_{2,t}) (v_b + v_t) + \frac{1}{2} gh_b h_t \end{bmatrix}. \tag{4.4}$$

The entropy conservative DG methods for two-dimensional SWEs (4.1) are given by

$$\begin{aligned} & \left(\frac{\partial \mathbf{Q}}{\partial t}, \omega \right)_\Omega + ((2D_h^x \mathbf{f}_S(\mathbf{Q}_e(x, y), \mathbf{Q}_e(\hat{x}, \hat{y})))|_{\hat{x}=x, \hat{y}=y}, \omega)_\Omega + \\ & ((2D_h^y \mathbf{g}_S(\mathbf{Q}_e(x, y), \mathbf{Q}_e(\hat{x}, \hat{y})))|_{\hat{x}=x, \hat{y}=y}, \omega)_\Omega + \begin{pmatrix} 0 \\ (gh_e D_h^x b_e, \omega)_\Omega \\ (gh_e D_h^y b_e, \omega)_\Omega \end{pmatrix} = 0, \end{aligned} \tag{4.5}$$

where \mathbf{Q}_e and b_e are given by

$$\mathbf{Q}_e = \mathbf{Q}(\mathbb{P}e) = \begin{bmatrix} h_e \\ m_{1,e} \\ m_{2,e} \end{bmatrix}, \quad h_e = \frac{1}{g} \left(\mathbb{P}e_1 + \frac{1}{2} ((\mathbb{P}e_2)^2 + (\mathbb{P}e_3)^2) - g\mathbb{P}b \right), \\ m_{1,e} = h_e \mathbb{P}e_2, \quad m_{2,e} = h_e \mathbb{P}e_3, \quad b_e = \mathbb{P}b.$$

The derivative operator D_h^y follows the same definition as D_h^x in (2.9), except the normal vector n_x is replaced by n_y . The expansion of the two-dimensional entropy stable DG methods (4.5), after plugging in the derivative operators D_h^x and the entropy conservative numerical fluxes (4.3) and (4.4), are listed in ‘‘Appendix A’’. For the proposed methods, we have the following theorem, which states that the nice properties of the one-dimensional methods also hold for the two-dimensional methods.

Theorem 7 *The two-dimensional method outlined in (4.5) for the SWEs is entropy conservative, locally conservative and well-balanced for still-water steady state solutions.*

The detailed proof is omitted here. It exactly follows the steps of those for the one-dimensional results, but becomes slightly more complicated due to the two-dimensional effects.

By adding additional dissipative terms at the element interfaces, as done for the one-dimensional case in (3.23), the semi-discrete entropy stable can also be derived and proven for two-dimensional problems. The two-dimensional positivity-preserving limiter [43,46] is given by

$$\tilde{\mathbf{Q}}_{ij}^n(x, y) = \theta \left(\mathbf{Q}_{ij}^n(x, y) - \overline{\mathbf{Q}}_{ij}^n \right) + \overline{\mathbf{Q}}_{ij}^n, \quad \theta = \min \left\{ 1, \frac{\overline{h}_{ij}^n}{h_{ij}^n - d_{ij}} \right\}, \tag{4.6}$$

where

$$\begin{aligned} d_{ij} &= \min_{(x,y) \in S_{ij}} h_{ij}^n(x, y), \\ S_{ij} &= \left\{ (x, y) : x \in S_i^x, y \in S_j^y, \text{ or } x \in S_i^x, y \in S_j^y \right\}. \end{aligned} \tag{4.7}$$

and the sets of one-dimensional Gauss–Lobatto quadrature points, denoted by $S_i^x = \{\hat{x}_i^r : r = 1, \dots, N\}$, $S_j^y = \{\hat{y}_j^r : r = 1, \dots, N\}$, are used. Again, this limiter does not affect the entropy stable property.

Table 1 L^1 errors and convergence rate of the entropy stable DG method for the test in Sect. 5.1

N	h		hu	
	L^1 error	Order	L^1 error	Order
25	5.55E-4		4.28E-3	
50	6.56E-5	3.08	5.65E-4	2.92
100	6.55E-6	3.32	5.58E-5	3.33
200	6.42E-7	3.35	5.48E-6	3.35
400	7.50E-8	3.10	6.43E-7	3.09
800	9.17E-9	3.03	8.45E-8	2.93

5 Numerical Experiments

In this section we present numerical results to demonstrate the performance of the proposed entropy stable and well-balanced DG methods. In addition to the well-balanced properties, we also demonstrate the positivity-preserving feature, high order accuracy, as well as other aspects. The third order DG method with quadratic polynomials is tested. For the two-dimensional problem, the tensor product polynomial space Q^2 is used as the solution space. For the explicit time discretization, the third order TVD Runge–Kutta method is applied. The gravitation constant g is taken as 9.812 and the CFL condition is taken as 0.18. The TVB slope limiter is implemented to eliminate the spurious oscillation, and in most numerical examples, the TVB constant M is set as 0 unless stated otherwise.

5.1 Accuracy Test

We start with an accuracy test to demonstrate the high order accuracy of our schemes for a smooth solution of the SWEs. Following the setup in [39], the bottom topography and initial conditions are:

$$\begin{cases} b(x) = \sin^2(\pi x), \\ h(x, 0) = 5 + e^{\cos(2\pi x)}, \\ hu(x, 0) = \sin(\cos(2\pi x)), \end{cases} \quad (5.1)$$

in the computational domain $[0, 1]$ with periodic boundary conditions. The final time is picked as $t = 0.1$, when the solution is still smooth. Since the exact solution is not known explicitly, we use the fifth order finite volume WENO scheme presented in [40] with 12,800 uniform cells to compute a reference solution, and compute the numerical errors by treating this reference solution as the exact solution. The TVB slope limiter procedure is turned off in this accuracy test. Table 1 shows the L^1 errors and order of accuracy of the numerical solutions, from which we can clearly see that, for the proposed entropy stable DG method, third order accuracy is achieved for this test. We have also tested the accuracy of the entropy conservative DG method (i.e., without adding the dissipation term), and the results are shown in Table 2, where again the third order convergence rate is observed as we refine the mesh.

5.2 The Well-Balanced Test

In this example, we test the well-balanced property of our proposed methods to ensure that the still-water steady state is exactly preserved. We consider two different choices of the

Table 2 L^1 errors and convergence rate of the entropy conservative DG method for the test in Sect. 5.1

N	h		hu	
	L^1 error	Order	L^1 error	Order
25	3.00E-3		2.77E-2	
50	3.34E-4	3.17	2.92E-3	3.25
100	1.05E-5	4.99	9.09E-5	5.00
200	5.71E-7	4.20	4.86E-6	4.22
400	7.22E-8	2.98	6.19E-7	2.98
800	9.01E-9	3.00	7.72E-8	3.00

Table 3 L^1 and L^∞ errors for the stationary solution with a smooth bottom, for the test in Sect. 5.2

N	L^1 error		L^∞ error	
	h	hu	h	hu
100	1.0E-13	5.8E-14	1.4E-13	2.9E-13
200	1.4E-13	9.1E-14	1.9E-13	4.1E-13
400	2.1E-13	1.1E-13	3.1E-13	4.9E-13

Table 4 L^1 and L^∞ errors for the stationary solution with a discontinuous bottom, for the test in Sect. 5.2

N	L^1 error		L^∞ error	
	h	hu	h	hu
100	1.1E-13	5.4E-14	1.5E-13	3.7E-13
200	1.1E-13	5.0E-14	1.6E-13	3.2E-13
400	1.2E-13	4.0E-14	1.7E-13	2.6E-13

bottom topography in the computational domain ($0 \leq x \leq 10$), with one being smooth

$$b(x) = 5 \exp\left(-\frac{2}{5}(x - 5)^2\right),$$

and the other being discontinuous

$$b(x) = \begin{cases} 4, & \text{if } 4 \leq x \leq 8, \\ 0, & \text{otherwise.} \end{cases}$$

The initial condition is taken as the stationary state

$$h + b = 10, \quad hu = 0,$$

which should be exactly preserved.

We solve the problem using double precision until the final time $t = 0.5$, with three different meshes of 100, 200 and 400 uniform elements. The L^1 error and L^∞ error for the water height h and the momentum hu are shown in Tables 3 and 4. We can observe that all the errors for both smooth and discontinuous bottom topography cases are at the level of roundoff errors, which verifies the well-balanced property.

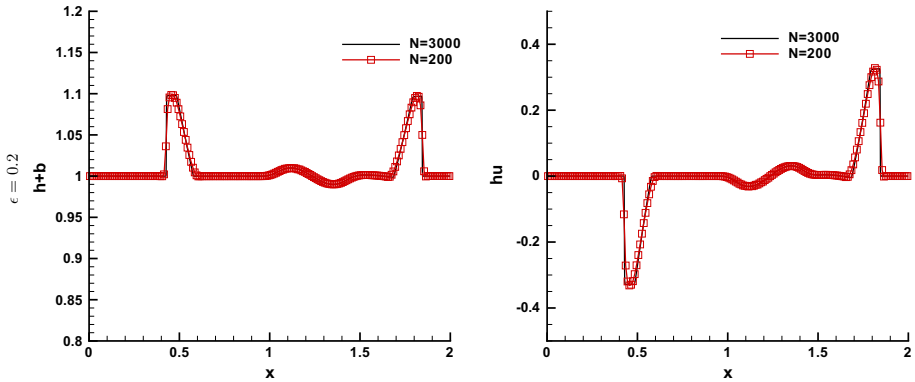


Fig. 2 A small perturbation test in Sect. 5.3, with a big pulse $\epsilon = 0.2$ at time $t = 0.2$. Left: the water surface $h + b$; right: the momentum hu

5.3 A Small Perturbation Test

To demonstrate the capability of the proposed DG methods in computing a rapidly varying flow over a smooth bed, we test the following quasi-stationary test case [28], which is a small perturbation of the steady state solution.

In the computational domain $[0, 2]$, the bottom topography $b(x)$ is given by

$$b(x) = \begin{cases} 0.25(\cos(10\pi(x - 1.5)) + 1), & \text{if } 1.4 \leq x \leq 1.6, \\ 0, & \text{otherwise,} \end{cases}$$

and the initial conditions of h and hu are

$$h(x, 0) = \begin{cases} 1 - b(x) + \epsilon, & \text{if } 1.1 \leq x \leq 1.2, \\ 1 - b(x), & \text{otherwise,} \end{cases} \quad hu(x, 0) = 0, \quad (5.2)$$

where ϵ is a given constant representing the size of the perturbation. Two cases with the big pulse ($\epsilon = 0.2$) and small pulse ($\epsilon = 0.001$) have been tested to the final stopping time $t = 0.2$, with simple transmissive boundary conditions. Theoretically, this perturbation splits into two waves, propagating to different direction. The small perturbation case with $\epsilon = 0.001$ is usually difficult to capture for non-well-balanced numerical methods.

The total water surface $h + b$ and momentum hu for the case with big pulse $\epsilon = 0.2$ and 200 uniform elements, compared with a reference solution with 3000 uniform element, are shown in Fig. 2. The same results for the case with small pulse $\epsilon = 0.001$ are shown in Fig. 3. At this time, the water pulse traveling to the right has already passed the bump. We can clearly observe that both cases are well resolved and the solutions do not have spurious numerical oscillations.

5.4 One-Dimensional Dam Breaking Problem

The one-dimensional dam breaking problem over a rectangular bump, considered in [39], is tested in this example. It involves a rapidly varying flow over a discontinuous bottom topography.

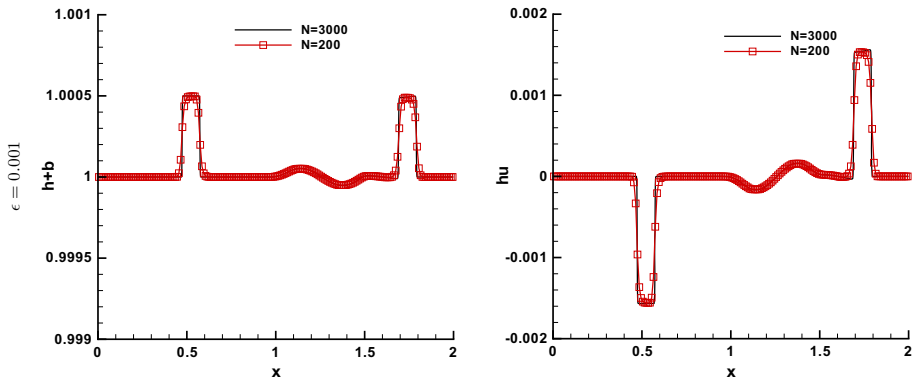


Fig. 3 A small perturbation test in Sect. 5.3, with a small pulse $\epsilon = 0.001$ at time $t = 0.2$. Left: the water surface $h + b$; right: the momentum hu

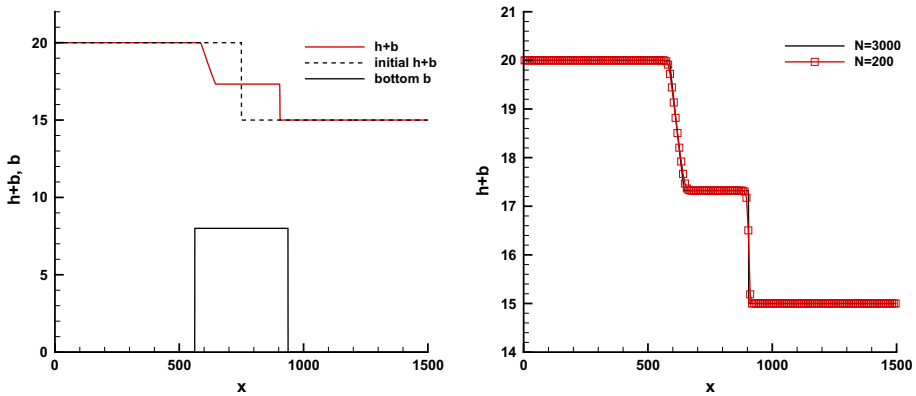


Fig. 4 The surface level $h + b$ for the dam breaking problem at $t = 15$, for the dam-breaking test in Sect. 5.4

The computational domain is set as $[0, 1500]$, and the discontinuous bottom topography takes the form of

$$b(x) = \begin{cases} 8, & \text{if } |x - 750| \leq 1500/8, \\ 0, & \text{otherwise.} \end{cases} \tag{5.3}$$

The initial conditions of h and hu are

$$h(x, 0) = \begin{cases} 20 - b(x), & \text{if } x \leq 750, \\ 15 - b(x), & \text{otherwise,} \end{cases} \quad u(x, 0) = 0. \tag{5.4}$$

We run the simulation until the final stopping time $t = 60$.

In this example, the water height h contains discontinuities at the points $x = 562.5$ and $x = 937.5$ (coming from the discontinuities of the bottom b), while the surface level $h + b$ is smooth there. In Figs. 4 and 5, the numerical results obtained with both 200 and 3000 uniform elements at two different ending times $t = 15$ and $t = 60$ are demonstrated. It is clear that the entropy stable DG scheme works well for this example, providing well-resolved, non-oscillatory solutions using 200 cells which agree well with the reference solutions using 3000 cells.

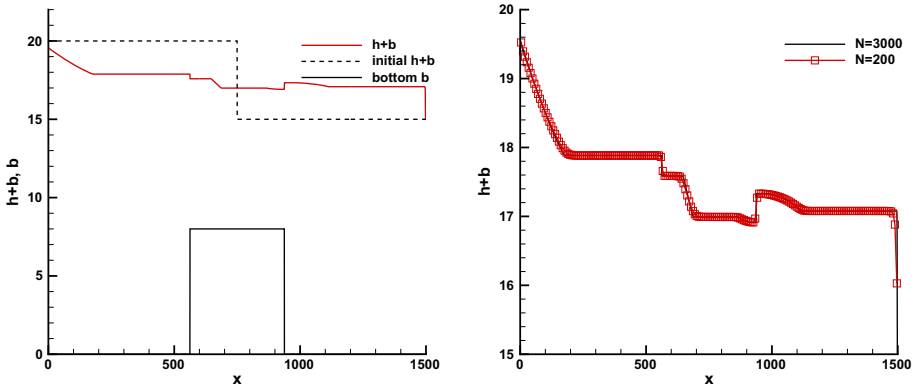


Fig. 5 The surface level $h + b$ for the dam breaking problem at $t = 60$, for the dam-breaking test in Sect. 5.4

5.5 Positivity-Preserving Test

The following dam-breaking test with a dried river bed is used to examine the positivity-preserving feature of the proposed DG method. The computational domain is set as $[-20, 20]$. Reflective boundary conditions are used, the bottom topography b is set as zero, and the initial conditions are given by

$$h(x, 0) = \begin{cases} 10, & \text{if } x \leq 0, \\ 0, & \text{otherwise,} \end{cases} \quad hu(x, 0) = 0.$$

The water surface level obtained with 100 uniform elements at time $t = 0.2$, $t = 0.5$ and $t = 1$ are shown in Fig. 6. The positivity-preserving limiter works well in avoiding the nonphysical negative water height. Without the use of the positivity-preserving limiter, this test case crashes immediately and cannot run unless something is done at the drying and wetting front.

5.6 Entropy Glitch Test

In this section, we follow the example studied in [36] and consider a specific dam-breaking problem to show the necessity of the entropy stable feature. It was shown in [36, Fig. 8] that standard DG method with a local Lax–Friedrichs numerical flux develops an unphysical discontinuity, called an “entropy glitch”, at $x = 0$, while the entropy stable method is able to capture the solution well on the coarse mesh.

The initial conditions are taken as

$$h(x, 0) = \begin{cases} 1.0, & \text{if } x \leq 0, \\ 0.1, & \text{otherwise,} \end{cases} \quad u(x, 0) = 0, \tag{5.5}$$

on the computational domain $[-1, 1]$, with the flat bottom $b = 0$. To match the setup in [36], we take the gravity constant g to be 10 and the final stopping time to be 0.2. 100 uniform elements are used, and the numerical results are shown in Fig. 7, where we can observe that no unphysical discontinuity appears near $x = 0$ and our entropy stable method does not produce the entropy glitch for this test.

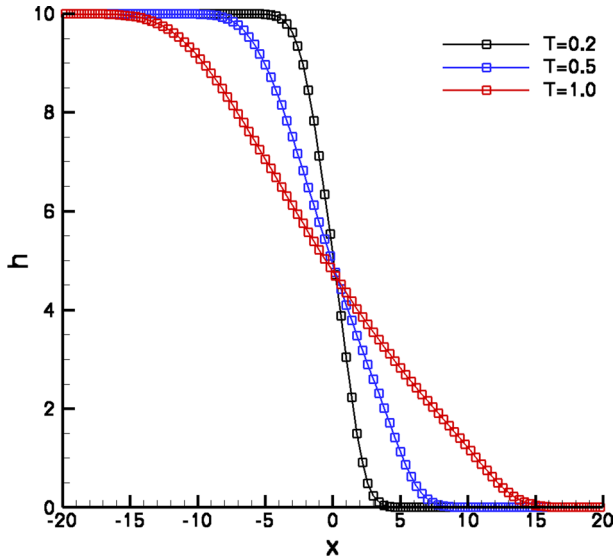


Fig. 6 The surface level $h + b$ for the dam breaking problem with a dried river bed in Sect. 5.5 at $t = 0.2$, $t = 0.5$ and $t = 1.0$

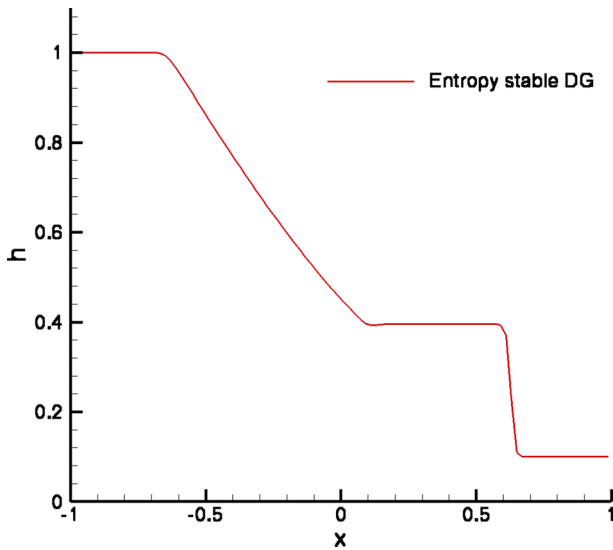


Fig. 7 The water height h for the entropy glitch test case in Sect. 5.6 at $t = 0.2$

5.7 Two-Dimensional Accuracy Test

We have also tested the proposed entropy stable DG methods on two-dimensional problem with rectangular meshes. This example is used to check the numerical accuracy of our two-dimensional methods. Following the setup in [39], the bottom topography and initial conditions are given by

Table 5 L^1 errors and numerical orders of accuracy for the test in Sect. 5.7

N	h		hu		hv	
	L^1 error	Order	L^1 error	Order	L^1 error	Order
25×25	3.00E-2		1.80E-1		2.49E-1	
50×50	7.31E-3	2.04	3.75E-2	2.26	5.77E-2	2.11
100×100	1.49E-3	2.29	7.71E-3	2.38	1.12E-2	2.40
200×200	2.88E-4	2.37	1.29E-4	2.48	2.02E-3	2.47

$$\begin{cases} b(x, y) = \sin(2\pi x) + \cos(2\pi y), \\ h(x, y, 0) = 10 + e^{\sin(2\pi x)} \cos(2\pi y), \\ hu(x, y, 0) = \sin(\cos(2\pi x)) \sin(2\pi y), \\ hv(x, y, 0) = \cos(2\pi x) \cos(\sin(2\pi y)), \end{cases} \tag{5.6}$$

in the computational domain $[0, 1] \times [0, 1]$, and periodic boundary conditions are used. The final time is set as $t = 0.05$. Since the exact solution is not known explicitly for this test case, we use the third order standard DG scheme with 800×800 rectangular meshes to compute a reference solution and compute the numerical errors. The TVB constant M is taken as 40 in this test, to avoid the reduction of accuracy near the extreme points. The L^1 errors and orders of accuracy are demonstrated in Table 5.

5.8 The Two-Dimensional Well-Balanced Test

The purpose of this example is to verify the well-balanced property of our DG methods to preserve the steady state solution in two dimensions. The rectangular computation domain $[0, 1] \times [0, 1]$ is used, and the non-flat bottom topography is given by

$$b(x, y) = 0.8 \exp\left(-50\left(x - \frac{1}{2}\right)^2 - 50\left(y - \frac{1}{2}\right)^2\right), \tag{5.7}$$

The initial condition is taken as the stationary solution

$$h(x, y, 0) = 1 - b(x, y), \quad hu(x, y, 0) = hv(x, y, 0) = 0, \tag{5.8}$$

and periodic boundary condition is used.

The flat water surface should be exactly preserved. We compute the solution until the final time $t = 0.1$ using double-precision, with three different meshes of 50×50 , 100×100 and 200×200 rectangular meshes. Table 6 shows the L^1 and L^∞ errors for the water height h (which is not a constant function) and the momentums hu, hv . We can observe that all the errors are at the level of roundoff errors, which verifies the well-balanced property.

5.9 A Small Perturbation of Two-Dimensional Steady State

In this section, we consider a classical example, studied by LeVeque [28], to demonstrate the capability of the proposed scheme in capturing a small perturbation of the stationary state. The computation domain is $[0, 2] \times [0, 1]$. The bottom topography consists of an elliptical shaped hump

$$b(x, y) = 0.8 \exp\left(-5(x - 0.9)^2 - 50(y - 0.5)^2\right), \tag{5.9}$$

Table 6 L^1 and L^∞ errors for the stationary solution, for the test in Sect. 5.8

$N \times M$	L^1 error			L^∞ error		
	h	hu	hv	h	hu	hv
50×50	1.2E-15	2.8E-15	2.5E-15	3.2E-11	3.1E-14	3.2E-14
100×100	9.4E-16	3.1E-15	3.0E-15	1.8E-11	3.4E-14	3.2E-14
200×200	6.6E-16	3.6E-15	3.7E-15	1.4E-11	3.7E-13	3.8E-14

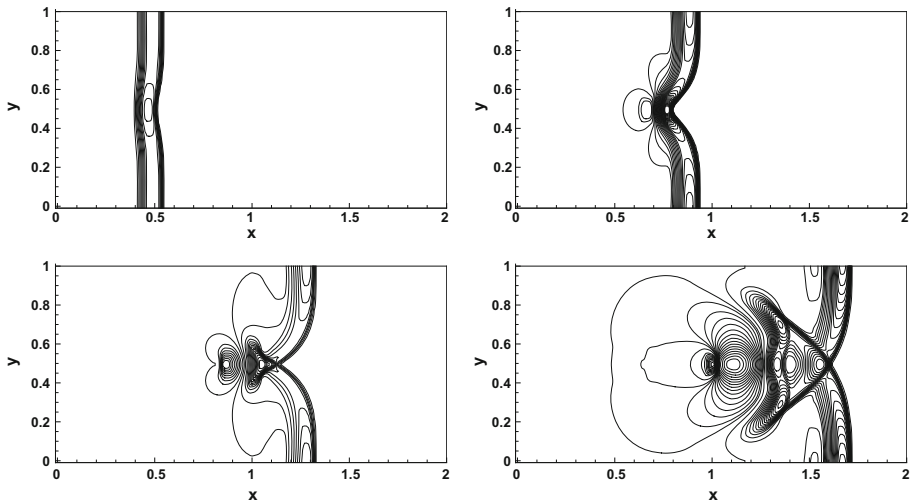


Fig. 8 The contours of the surface level $h + b$ for the small perturbation problem in Sect. 5.9 at times $t = 0.12, t = 0.24, t = 0.36$ and $t = 0.48$ with 200×100 uniform meshes

and the initial conditions of h, hu and hv are

$$h(x, y, 0) = \begin{cases} 1 - b(x, y) + 0.01, & \text{if } 0.05 \leq x \leq 0.15, \\ 1 - b(x, y), & \text{otherwise,} \end{cases}$$

$$hu(x, y, 0) = hv(x, y, 0) = 0,$$

which means that the surface is almost flat except for the region $0.05 \leq x \leq 0.15$, where h is perturbed by a size of 0.01. Figure 8 displays the surface level $h + b$ at different times $t = 0.24, t = 0.36$ and $t = 0.48$ with 200×100 uniform meshes. We can see that the right-going disturbance propagates past the hump naturally, and the complex small features of the flow can be resolved very well.

5.10 Oblique Two-Dimensional Dam Break

In this section, we consider a two-dimensional dam break problem, studied in [3,42]. In the computational domain $[-0.5, 0, 5] \times [-0.5, 0, 5]$, the initial condition is set as

$$h(x, y, 0) = \begin{cases} 1 & \text{if } x + y \leq 0, \\ 0 & \text{otherwise} \end{cases}, \quad \text{and} \quad hu(x, y, 0) = hv(x, y, 0) = 0, \quad (5.10)$$

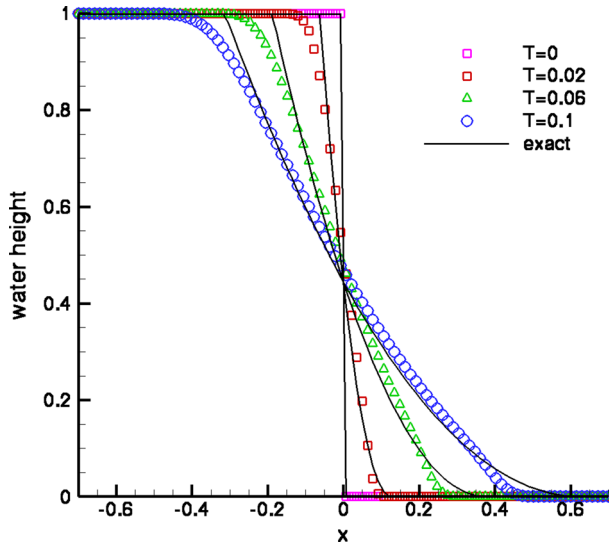


Fig. 9 Oblique 2D dam break problem in Sect. 5.10. Surface level at different times in the central cross section

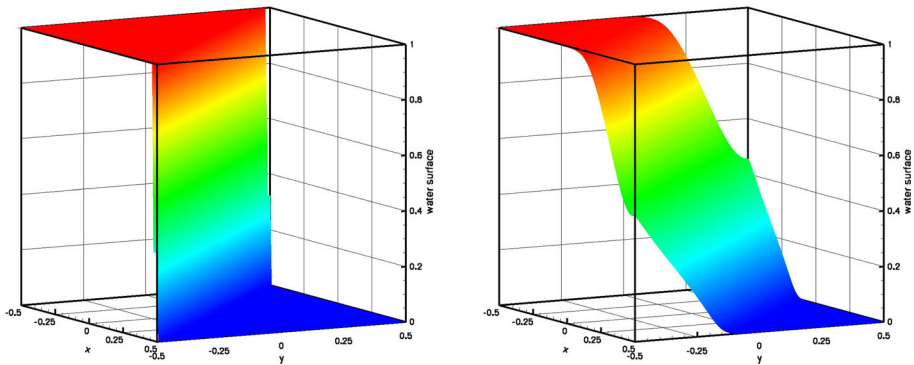


Fig. 10 Oblique 2D dam break problem in Sect. 5.10. The surface level at $t = 0$ (left) and $t = 0.06$ (right)

with the flat bottom $b = 0$. Still water appears in half of the area, and dry areas appear in the other half. This produces a moving front which inclines 45° to the boundary of the domain.

The analytic solution of this test is available in [5]. The comparison of the numerical results and the analytical solutions is provided in Fig. 9, for the surface elevations on the central cross section (the $x = y$ plane) at different times $t = 0, 0.02, 0.06$ and 0.1 with 100×100 uniform cells. Figure 10 shows the three-dimensional plot of the initial surface and the water surface at $t = 0.6$. We can observe a good agreement between the numerical and analytical solutions, and the positivity-preserving limiter works well in avoiding the nonphysical negative water height.

6 Conclusion

In this work, we present entropy stable, well-balanced and positivity-preserving DG methods for the nonlinear SWEs with a non-flat bottom topography. The entropy stable property, local conservation, well-balanced property and positivity-preserving feature are validated for the one-dimensional method, and these proofs could be easily extended to two dimensions on rectangular meshes. Both one- and two-dimensional numerical results are provided to demonstrate the performance of the proposed DG methods. Only the rectangular meshes in two-dimensional setting are considered in this paper as a first step to illustrate the idea, and our future work involves the extension of these methods to curvilinear grids and triangular grids, when domain with complex geometry is considered.

Acknowledgements The work of X. Wen is supported by the China Scholarship Council fellowship. The work of Y. Xing is partially sponsored by NSF Grant DMS-1753581. The work of X. Wen, Z. Gao and W.S. Don is partially supported by the National Natural Science Foundation of China (11871443), Shandong Provincial Natural Science Foundation (ZR2017MA016), and Shandong Provincial Qingchuang Science and Technology Project (2019KJ1002). W.S. Don also likes to thank the Ocean University of China for providing the startup funding (201712011) that is used in supporting this work.

Data Availability The datasets generated during and/or analyzed during the current study are available from the corresponding author on reasonable request.

Appendix A: Two-Dimensional DG Methods

The two-dimensional entropy stable DG methods (4.5), after following the definition of the derivative operators D_h^x in Definition 3 and the entropy conservative numerical fluxes (4.3) and (4.4), can be expanded as

$$\left\{ \begin{aligned} & \sum_k \left(\frac{\partial h}{\partial t}, \omega \right)_{\Omega^k} + \left(\frac{\partial \mathbb{P}m_{1,e}}{\partial x} + \frac{\partial \mathbb{P}m_{2,e}}{\partial y}, \omega \right)_{\Omega^k} \\ & + \left\langle f_S^{(1)}(Q_e^+, Q_e) - \mathbb{P}m_{1,e}, \omega n_x \right\rangle_{\partial\Omega^k} + \left\langle g_S^{(1)}(Q_e^+, Q_e) - \mathbb{P}m_{2,e}, \omega n_y \right\rangle_{\partial\Omega^k} = 0, \\ & \sum_k \left(\frac{\partial m_1}{\partial t}, \omega \right)_{\Omega^k} + \left(\frac{1}{2} \frac{\partial}{\partial x} (\mathbb{P}m_{1,e} u_e) + \frac{1}{2} u_e \frac{\partial}{\partial x} (\mathbb{P}m_{1,e}) + \frac{1}{2} m_{1,e} \frac{\partial}{\partial x} u_e + g h_e \frac{\partial}{\partial x} (\mathbb{P}h_e), \omega \right)_{\Omega^k} \\ & + \left(g h_e \frac{\partial}{\partial x} b_e, \omega \right)_{\Omega^k} + \left(\frac{1}{2} \frac{\partial}{\partial y} (\mathbb{P}m_{2,e} u_e) + \frac{1}{2} u_e \frac{\partial}{\partial y} (\mathbb{P}m_{2,e}) + \frac{1}{2} m_{2,e} \frac{\partial}{\partial y} u_e, \omega \right)_{\Omega^k} \\ & + \left\langle f_S^{(2)}(Q_e^+, Q_e) + \text{I}, \omega n_x \right\rangle_{\partial\Omega^k} + \text{V} + \left\langle g_S^{(2)}(Q_e^+, Q_e) + \text{II}, \omega n_y \right\rangle_{\partial\Omega^k} + \text{VI} = 0, \\ & \sum_k \left(\frac{\partial m_2}{\partial t}, \omega \right)_{\Omega^k} + \left(\frac{1}{2} \frac{\partial}{\partial x} (\mathbb{P}m_{1,e} v_e) + \frac{1}{2} v_e \frac{\partial}{\partial x} (\mathbb{P}m_{1,e}) + \frac{1}{2} m_{1,e} \frac{\partial}{\partial x} v_e, \omega \right)_{\Omega^k} \\ & + \left(\frac{1}{2} \frac{\partial}{\partial y} (\mathbb{P}m_{2,e} v_e) + \frac{1}{2} v_e \frac{\partial}{\partial y} (\mathbb{P}m_{2,e}) + v \frac{1}{2} m_{2,e} \frac{\partial}{\partial y} v_e + g h_e \frac{\partial}{\partial y} (\mathbb{P}h_e), \omega \right)_{\Omega^k} + \left(g h_e \frac{\partial}{\partial y} b_e, \omega \right)_{\Omega^k} \\ & + \left\langle f_S^{(3)}(Q_e^+, Q_e) + \text{III}, \omega n_y \right\rangle_{\partial\Omega^k} + \text{VII} + \left\langle g_S^{(3)}(Q_e^+, Q_e) + \text{IV}, \omega n_x \right\rangle_{\partial\Omega^k} + \text{VIII} = 0, \end{aligned} \right.$$

with the terms I - VIII defined by

$$\begin{aligned} \text{I} &= \Phi(m_{1,e}, u_e) - \frac{1}{2}gh_e(\mathbb{P}h_e - \llbracket b_e \rrbracket), & \text{II} &= \Phi(m_{2,e}, u_e), \\ \text{III} &= \Phi(m_{1,e}, v_e), & \text{IV} &= \Phi(m_{2,e}, v_e) - \frac{1}{2}gh_e(\mathbb{P}h_e - \llbracket b_e \rrbracket), \\ \text{V} &= \frac{1}{4}\Psi_x(m_{1,e}, u_e) + \frac{1}{2}g\Psi_x(h_e, h_e), & \text{VI} &= \frac{1}{4}\Psi_x(m_{2,e}, u_e), \\ \text{VII} &= \frac{1}{4}\Psi_y(m_{1,e}, v_e), & \text{VIII} &= \frac{1}{4}\Psi_y(m_{2,e}, v_e) + \frac{1}{2}g\Psi_y(h_e, h_e), \end{aligned}$$

where the notations

$$\begin{aligned} \Phi(a, b) &= -\frac{1}{2}\mathbb{P}(ab) + \frac{1}{4}(\mathbb{P}a + a)b, & \Psi_x(a, b) &= \langle \mathcal{E}(a), \mathbb{P}(bw)n_x \rangle_{\partial\Omega^k}, & \Psi_y(a, b) \\ &= \langle \mathcal{E}(a), \mathbb{P}(bw)n_y \rangle_{\partial\Omega^k}, \end{aligned}$$

are used. An equivalent form of the DG methods, which uses the vector variables and local matrices to guide the efficient implementation, is available in [9].

References

1. Audusse, E., Bouchut, F., Bristeau, M.O., Klein, R., Perthame, B.: A fast and stable well-balanced scheme with hydrostatic reconstruction for shallow water flows. *SIAM J. Sci. Comput.* **25**, 2050–2065 (2004)
2. Bale, D.S., LeVeque, R.J., Mitran, S., Rossmannith, J.A.: A wave propagation method for conservation laws and balance laws with spatially varying flux functions. *SIAM J. Sci. Comput.* **24**, 955–978 (2002)
3. Berthon, C., Marche, F.: A positive preserving high order VFRoe scheme for shallow water equations: a class of relaxation schemes. *SIAM J. Sci. Comput.* **30**, 2587–2612 (2008)
4. Bermudez, A., Vazquez, M.E.: Upwind methods for hyperbolic conservation laws with source terms. *Comput. Fluids* **23**, 1049–1071 (1994)
5. Bokhove, O.: Flooding and drying in discontinuous Galerkin finite-element discretizations of shallow-water equations. Part I: one dimension. *J. Sci. Comput.* **22**, 47–82 (2005)
6. Bollermann, A., Noelle, S., Lukáčová-Medviová, M.: Finite volume evolution Galerkin methods for the shallow water equations with dry beds. *Commun. Comput. Phys.* **10**, 371–404 (2010)
7. Bunya, S., Kubatko, E.J., Westerink, J.J., Dawson, C.: A wetting and drying treatment for the Runge–Kutta discontinuous Galerkin solution to the shallow water equations. *Methods Appl. Mech. Eng.* **198**, 1548–1562 (2009)
8. Carpenter, M., Fisher, T., Nielsen, E., Frankel, S.: Entropy stable spectral collocation schemes for the Navier–Stokes equations: discontinuous interfaces. *SIAM J. Sci. Comput.* **36**(5), B835–B867 (2014)
9. Chan, J.: On discretely entropy conservative and entropy stable discontinuous Galerkin methods. *J. Comput. Phys.* **362**, 346–374 (2018)
10. Chan, J.: On discretely entropy conservative and entropy stable discontinuous Galerkin methods. [arXiv:1708.01243v4](https://arxiv.org/abs/1708.01243v4) [math.NA]
11. Chen, T., Shu, C.-W.: Entropy stable high order discontinuous Galerkin methods with suitable quadrature rules for hyperbolic conservation laws. *J. Comput. Phys.* **345**, 427–461 (2017)
12. Chen, T., Shu, C.-W.: Review of entropy stable discontinuous Galerkin methods for systems of conservation laws on unstructured simplex meshes. *CSIAM Trans. Appl. Math. (CSAM)* (2020). <https://doi.org/10.4208/csiam-am.2020-0003>
13. Cockburn, B., Karniadakis, G., Shu, C.-W.: The development of discontinuous Galerkin methods. In: Cockburn, B., Karniadakis, G., Shu, C.-W. (eds.) *Discontinuous Galerkin Methods: Theory, Computation and Applications*. Lecture Notes in Computational Science and Engineering, Part I: Overview, vol. 11, pp. 5–50. Springer, New York (2000)
14. Cockburn, B., Shu, C.-W.: TVB Runge–Kutta local projection discontinuous Galerkin finite element method for conservation laws II: general framework. *Math. Comput.* **52**, 411–435 (1989)
15. Cockburn, B., Shu, C.-W.: The Runge–Kutta discontinuous Galerkin method for conservation laws V: multidimensional systems. *J. Comput. Phys.* **141**, 199–224 (1998)

16. Dawson, C., Proft, J.: Discontinuous and coupled continuous/discontinuous Galerkin methods for the shallow water equations. *Comput. Methods Appl. Mech. Eng.* **191**, 4721–4746 (2002)
17. Eskilsson, C., Sherwin, S.J.: A triangular spectral/hp discontinuous Galerkin method for modelling 2D shallow water equations. *Int. J. Numer. Methods Fluids* **45**, 605–623 (2004)
18. Ern, A., Piperno, S., Djadel, K.: A well-balanced Runge–Kutta discontinuous Galerkin method for the shallow-water equations with flooding and drying. *Int. J. Numer. Methods Fluids* **58**, 1–25 (2008)
19. Fjordholm, U.S., Mishra, S., Tadmor, E.: Well-balanced and energy stable schemes for the shallow water equations with discontinuous topography. *J. Comput. Phys.* **230**, 5587–5609 (2011)
20. Gallardo, J.M., Parés, C., Castro, M.: On a well-balanced high-order finite volume scheme for shallow water equations with topography and dry areas. *J. Comput. Phys.* **227**, 574–601 (2007)
21. Gassner, G.J.: A skew-symmetric discontinuous Galerkin spectral element discretization and its relation to SBP-SAT finite difference methods. *SIAM J. Sci. Comput.* **35**, A1233–A1253 (2013)
22. Gassner, G.J., Winters, A.R., Kopriva, D.A.: A well balanced and entropy conservative discontinuous Galerkin spectral element method for the shallow water equations. *Appl. Math. Comput.* **272**, 291–308 (2016)
23. Giraldo, F.X., Hesthaven, J.S., Warburton, T.: Nodal high-order discontinuous Galerkin methods for the spherical shallow water equations. *J. Comput. Phys.* **181**, 499–525 (2002)
24. Hesthaven, J.S., Warburton, T.: *Nodal Discontinuous Galerkin Methods: Algorithms, Analysis, and Applications*. Springer, Berlin (2007)
25. Hou, S., Liu, X.-D.: Solutions of multi-dimensional hyperbolic systems of conservation laws by square entropy condition satisfying discontinuous Galerkin method. *J. Sci. Comput.* **31**, 127–151 (2007)
26. Kopriva, D.A., Gassner, G.: On the quadrature and weak form choices in collocation type discontinuous Galerkin spectral element methods. *J. Sci. Comput.* **44**, 136–155 (2010)
27. Kurganov, A., Levy, D.: Central-upwind schemes for the Saint–Venant system. *Math. Model. Numer. Anal.* **36**, 397–425 (2002)
28. LeVeque, R.J.: Balancing source terms and flux gradients on high-resolution Godunov methods: the quasi-steady wave-propagation algorithm. *J. Comput. Phys.* **146**, 346–365 (1998)
29. Perthame, B., Simeoni, C.: A kinetic scheme for the Saint–Venant system with a source term. *Calcolo* **38**, 201–231 (2001)
30. Ranocha, H.: Shallow water equations: split-form, entropy stable, well-balanced, and positivity preserving numerical methods. *Int. J. Geomath.* **8**, 85–133 (2017)
31. Schwanenberg, D., Königeter, J.: A discontinuous Galerkin method for the shallow water equations with source terms. In: Cockburn, B., Karniadakis, G., Shu, C.-W. (eds.) *Discontinuous Galerkin Methods: Theory, Computation and Applications*. Lecture Notes in Computational Science and Engineering, Part I: Overview, pp. 289–309. Springer, Berlin (2000)
32. Tadmor, E.: The numerical viscosity of entropy stable schemes for systems of conservation laws I. *Math. Comput.* **49**(1987), 91–103 (1987)
33. Tadmor, E.: Entropy stability theory for difference approximations of nonlinear conservation laws and related time-dependent problems. *Acta Numer.* **12**, 451–512 (2003)
34. Tadmor, E.: Entropy stable schemes. In: Abgrall, R., Shu, C.-W. (eds.) *Handbook of Numerical Methods for Hyperbolic Problems*, vol. XVII, pp. 467–493. Elsevier, London (2016)
35. Wen, X., Gao, Z., Don, W.S., Xing, Y., Li, P.: Application of positivity-preserving well-balanced discontinuous Galerkin method in computational hydrology. *Comput. Fluids* **139**, 112–119 (2016)
36. Wintermeyer, N., Winters, A.R., Gassner, G.J., Warburton, T.: An entropy stable discontinuous Galerkin method for the shallow water equations on curvilinear meshes with wet/dry fronts accelerated by GPUs. *J. Comput. Phys.* **375**, 447–480 (2018)
37. Wintermeyer, N., Winters, A.R., Gassner, G.J., Kopriva, D.A.: An entropy stable nodal discontinuous Galerkin method for the two dimensional shallow water equations on unstructured curvilinear meshes with discontinuous bathymetry. *J. Comput. Phys.* **340**, 200–227 (2017)
38. Xing, Y.: Exactly well-balanced discontinuous Galerkin methods for the shallow water equations with moving water equilibrium. *J. Comput. Phys.* **257**, 536–553 (2014)
39. Xing, Y., Shu, C.-W.: High order finite difference WENO schemes with the exact conservation property for the shallow water equations. *J. Comput. Phys.* **208**, 206–227 (2005)
40. Xing, Y., Shu, C.-W.: High order well-balanced finite volume WENO schemes and discontinuous Galerkin methods for a class of hyperbolic systems with source terms. *J. Comput. Phys.* **214**, 567–598 (2006)
41. Xing, Y., Shu, C.-W.: A new approach of high order well-balanced finite volume WENO schemes and discontinuous Galerkin methods for a class of hyperbolic systems with source terms. *Commun. Comput. Phys.* **1**, 100–134 (2006)
42. Xing, Y., Shu, C.-W.: High-order finite volume WENO schemes for the shallow water equations with dry states. *Adv. Water Resour.* **34**, 1026–1038 (2011)

43. Xing, Y., Zhang, X., Shu, C.-W.: Positivity-preserving high order well-balanced discontinuous Galerkin methods for the shallow water equations. *Adv. Water Resour.* **33**, 1476–1493 (2010)
44. Xing, Y., Zhang, X.: Positivity-preserving well-balanced discontinuous Galerkin methods for the shallow water equations on unstructured triangular meshes. *J. Sci. Comput.* **57**, 19–41 (2013)
45. Xing, Y., Shu, C.-W.: A survey of high order schemes for the shallow water equations. *J. Math. Study* **47**, 221–249 (2014)
46. Zhang, X., Shu, C.-W.: On maximum-principle-satisfying high order schemes for scalar conservation laws. *J. Comput. Phys.* **229**, 3091–3120 (2010)

Publisher's Note Springer Nature remains neutral with regard to jurisdictional claims in published maps and institutional affiliations.